

# University of Chester



**This work has been submitted to ChesterRep – the University of Chester’s  
online research repository**

<http://chesterrep.openrepository.com>

Author(s): Henk Joseph du Preez

Title: A comparison of cyclic fatigue failure of two nickel titanium rotary endodontic file systems that use different manufacturing methods: a ground file (RaCe™) and a new innovative controlled memory file (HyFlex CM™) in a simulated root canal

Date: March 2014

Originally published as: University of Chester MSc dissertation

Example citation: du Preez, H. J. (2014). *A comparison of cyclic fatigue failure of two nickel titanium rotary endodontic file systems that use different manufacturing methods: a ground file (RaCe™) and a new innovative controlled memory file (HyFlex CM™) in a simulated root canal.* (Unpublished master’s thesis). University of Chester, United Kingdom.

Version of item: Amended version

Available at: <http://hdl.handle.net/10034/336544>

A comparison of cyclic fatigue failure of two nickel titanium rotary endodontic file systems that use different manufacturing methods: a ground file (RaCe™) and a new innovative controlled memory file (HyFlex CM™) in a simulated root canal

Henk Joseph du Preez

Student Number:

Assessment Number

Dissertation submitted to the University of Chester for the Degree of Master of Science in Endodontology

Word Count: 15960

March 2014

## **Abstract**

### Research Question

Do controlled memory nickel titanium rotary endodontic files have greater resistance to cyclic fatigue than ground nickel titanium files , in vitro, at test temperatures near those encountered clinically?

### Context and previous research

Controlled memory rotary files became available in 2010. Two in vitro research papers testing their resistance to cyclic fatigue against ground files have been published to date. These studies conducted their research at room temperature using a three pin bending device to rotate the files around a curvature. They both had sample sizes of twelve files per group. Controlled memory files performed significantly ( $p < 0.05$ ) better than ground files.

### Sample and setting

Forty seven HyFlexCM™ and forty eight RaCe™ files, both with a tip size of .25mm and constant taper of 6% were randomly acquired for comparison. The HyFlexCM™ files were sponsored by the manufacturer, the RaCe™ files were purchased from a U.K supplier. Both groups were run to failure at 500 revolutions per minute in an oil lubricated artificial canal constructed from hardened steel using electrical discharge sinking. The artificial canal tapered at 6%, from .35mm to 1.37mm with a 5mm radius of curvature and 90° bend in one plane. The test temperature was  $35 \pm 1$  °C.

### Data collection and Analysis

Raw data, in seconds to failure, was recorded by the author and converted to number of rotations to failure. Significance level was set at .05. Statistical analysis was performed with

SPSS™ statistical software. The Cox survival model was used to determine if there was a significant difference in the number of rotations to failure for each group.

### Findings

There was no statistically significant difference between the two groups.

### Conclusion

Controlled memory rotary endodontic files may be more likely to fail through cyclic fatigue when tested at clinically relevant temperatures rather than at room temperature as in previous studies.

## **Declaration**

The work is original and has not been submitted previously in support of any qualification or course.

## **Acknowledgements**

I would like to thank Dr Benjamin Ezeh at Coltène/Whaledent in Germany for kindly arranging the sponsorship of the HyFlexCM™ rotary nickel titanium files used for this dissertation. Coltène/Whaledent also kindly sponsored the cost of machining the steel cyclic fatigue test block.

I wish to thank Dr Michael Horrocks and Dr Mark Hunter for their invaluable and patient mentorship throughout my endodontology post graduate education. I wish to thank Dr Michael Horrocks as well for his help and advice in bringing this dissertation to fruition.

I would like to thank statistician, Dr Ola Badawi for her help with the statistical analysis.

I would also like to thank the staff at Waveney Precision for their help with machining the test block.

## **Table of contents**

Abstract.....	i
Declaration.....	iv
Acknowledgements.....	v
List of abbreviations.....	ix
List of figures.....	x
List of tables.....	xii
Chapters	
1) Introduction.....	1
2) Background.....	4
2.1) Endodontic instrumentation and its goals.....	4
2.2) NiTi Flexibility.....	7
2.3) Heat treatment of rotary NiTi instruments.....	9
2.4) NiTi phases and characteristic temperatures.....	12
2.5) NiTi wire manufacture .....	16
3) Literature review.....	19
3.1) Thermo-elastic martensitic transformation.....	21
3.2) Types of fatigue failure of rotary NiTi instruments.....	26
3.3) Comparison of properties of superelastic and CM NiTi wires.....	28
3.4) Behaviour of NiTi under cyclic loading.....	30
3.5) Mechanism of cyclic fatigue failure.....	32
3.6) Clinical and test factors that influence number of cycles to failure ( $N_f$ ).....	33

3.7) Rotary NiTi surface improvements to reduce cyclic fatigue failure.....	36
3.8) Thermal modification of rotary NiTi files to increase flexibility.....	38
3.9) Cyclic fatigue tests of CM wire to-date.....	40
4) Research Design.....	42
4.1) Theoretical Basis.....	42
4.2) Hypothesis testing.....	43
4.3) Validity.....	44
4.3.1) Instrument related confounds.....	45
4.3.2) Test related confounds.....	48
4.4) Data analysis.....	50
4.5) Reliability.....	51
4.6) Experimental method.....	52
4.7) Limitations of the experimental method.....	58
4.7.1) Limitations pertaining to internal validity.....	58
4.7.2) Limitations pertaining to external validity.....	60
5) Results.....	62
5.1) Descriptive and inferential statistics.....	62
5.2) Cox survival results and Kaplan Meier plots.....	65
5.3) Objective power.....	70
5.4) Discussion of results.....	71
6) Conclusion.....	72
7) Recommendations.....	75



References.....	77
Appendix A Data sheet for BA2 tool steel.....	85
Appendix B Geometry of the artificial canal.....	86
Appendix C Data sheet.....	87

## **List of abbreviations**

A <sub>f</sub>	Austenite finish temperature
A <sub>s</sub>	Austenite start temperature
BFR	Bend and free recovery
CM	Controlled Memory
DSC	Differential scanning calorimetry
M <sub>d</sub>	Thermal limit to elastic deformation of stress induced martensite
M <sub>f</sub>	Martensite finish temperature
M <sub>s</sub>	Martensite start temperature
MR	Martensite reorientation
N <sub>f</sub>	Number of rotations to failure
NiTi	Nickel Titanium
RaCe	Reamer with alternating cutting edges
SE	Superelasticity
SIM	Stress induced martensite
SMA	Shape memory alloys
UTS	Ultimate tensile strength

## **List of figures**

Figure 1. Root of a tooth demonstrating ideal root canal shaping goals.

Figure 2. Common apical preparation errors.

Figure 3. A stiff endodontic file straightens the outer curvature of the canal.

Figure 4. A Rotary NiTi file displaying the superelastic property.

Figure 5. A generalised stress - strain curve for stainless steel and superelastic NiTi under tensile load.

Figure 6. At a molecular level, the superelastic property is illustrated.

Figure 7. Stress Vs. strain curve for “as drawn” wire and wire that has been subject to different heat treatment processes.

Figure 8. Machining grooves on a HyFlexCM™ rotary NiTi file.

Figure 9. Hysteresis of the martensitic transformation.

Figure 10.  $A_f$  in degrees Celsius plotted against nickel content.

Figure 11. Basic methods for plastic deformation of shape memory alloys.

Figure 12. Thermo-elastic martensitic transformation.

Figure 13. A HyFlexCM™ file recovers shape when placed on hand.

Figure 14. Crystalline and micro structural forms of NiTi.

Figure 15. Tensile stress on superelastic NiTi wire,  $A_f = 6^\circ\text{C}$ .

Figure 16. Unwinding of a rotary NiTi file due to torque overload.

Figure 17. Graphic representation of compression and tension in a cylindrical wire as it rotates around a curve.

Figure 18. Comparison of tensile failure stress-strain plots of superelastic wire ( $A_f = 31 \pm 3.6^\circ\text{C}$ ) with CM wire ( $A_f = 48 \pm 3.9^\circ\text{C}$ ).

Figure 19. Comparison of stress-strain load-unload plot for CM and Superelastic (SE) wire of different diameter but performed only at room temperature.

Figure 20. Thermal martensite (analogous to CM wire) cycling at constant strain of  $\pm 2.5\%$ .

Figure 21. Examples of devices that do not restrict instruments with different bending properties to the same test trajectory.

Figure 22. A good agreement between artificial canal shape and file shape.

Figure 23. A Scientific Method flowchart.

Figure 24. Fractured RaCe™ file on left and HyFlexCM™ on right, both have a triangular cross section.

Figure 25. The artificial canal in the steel block.

Figure 26. Vice and G clamp assembly to connect allan key to test block.

Figure 27. The acrylic jig secure on the handpiece. The nut in the jig accommodates the vertical stop screw.

Figure 28. The full test assembly with vertical stop screw and locking nut.

Figure 29. Normal Q-Q plots for HyFlex and RaCe groups.

Figure 30. Box plots of  $N_f$  for each group.

Figure. 31 Histograms overlaid with normal plots for both file groups.

Figure 32. Kaplan-Meier survival curve of number of rations before failure.

Figure 33. Kaplan-Meier survival curve of at low number of rotations (less than 110).

Figure 34. Kaplan-Meier survival curve at high number of rotations (110 and higher).

Figure 35. PDF showing start and finish width of the canal.

Figure 36. Annotated CAD screenshot of the data used to manufacture the copper die for electrical discharge machining of the BA2 steel block to a depth of 2mm.

## **List of tables**

Table 1. Rotary NiTi manufacturing processes with some examples of rotary systems and the year the materials were introduced.

Table 2. Transformational temperatures for HyFlexCM™ files as determined by differential scanning calorimetry.

Table 3. Transformation temperatures for different rotary NiTi systems.

Table 4. Key search words and results.

Table 6. Descriptive stats of the data.

Table 7. Tests of normality.

Table 8. Results of Cox survival model.

Table 9. Results of Cox survival model using bootstrapping.

Table 10. Results of Cox survival model for low rotations (less than 110).

Table 11. Results of Cox survival model using bootstrapping for low rotations (less than 110).

Table 12. Results of Cox survival model for high rotations (110 and more).

Table 13. Results of Cox survival model using bootstrapping for high rotations (110 and more).

Table 14. Rockwell C Scale hardness of BA2 tool steel.

Table 15. Conversion table for Rockwell Hardness C to Vickers Hardness.

## **1. Introduction**

Nickel Titanium (NiTi) alloy has unique properties that have allowed it to be included in a limited list of so-called exotic or smart materials. These materials have one or more properties that can be significantly changed in a controlled manner by external stimuli (McCabe, Yan, Al Naimi, Mahmoud & Rolland, 2011). Nickel titanium, for example, can suffer large deformations (strains) that can be induced or recovered through temperature or stress (shape) change. Some properties of this material have led it to being favoured as the material of choice from which to make rotary nickel titanium endodontic instruments, in particular its superelastic qualities. These instruments have been in use since the early 1990's.

This material has provided several benefits including speed and efficiency of root canal preparation (Gutmann & Gao, 2012). However, there is a risk of fracture of these instruments inside the root canal. The perceived poor prognosis that will follow has led to a great deal of research to be carried out to help understand instrument fracture so that it can be prevented rather than treated (Parashos & Messer, 2006). In recent years manufacturers have been manipulating NiTi found in ground instruments primarily through heat treatment processes, in an attempt to enhance its ability to attain the goals that an ideal shaping instrument should be capable of providing. The most recent of these innovations is "controlled memory" (CM) nickel titanium files, introduced in 2010 (Shen, Zhou, Zheng, Peng & Haapasalo, 2013).

Very little research has been conducted on files made from this material. However, manufacturers claim that they are many times more fracture resistant than ground

instruments. One of the manufacturers that have made these claims is Coltène/Whaledent (Altstätten, Switzerland). They claim that their product, HyFlexCM™, is 300% more resistant to fracture than ground rotary NiTi files ([www.coltene.com](http://www.coltene.com)), therefore there seems to be a need to investigate these claims.

The rationale for using rotary NiTi instruments in endodontics necessitates a brief explanation of its metallurgical characteristics and manufacturing processes. This information will be covered in the background chapter which will also help develop an understanding of the recent advances in rotary NiTi technology.

In order to appreciate the development and place of controlled memory rotary NiTi files in the endodontic armamentarium, it will be important to mention the two other recent rotary NiTi systems; Twisted File™ (R phase technology) and M-Wire™. These two developments along with CM technology form what has become known as the second generation of rotary NiTi systems. Their distinguishing characteristic is that their manufacturing processes make use of heat treatments in a way that earlier ground rotary NiTi files did not. It has become necessary for clinicians to appreciate the nature of the raw materials used to make these NiTi instruments as well as their relevant mechanical properties (Zhou, Shen, Zheng, Zheng & Haapasalo, 2012).

A review of the literature will explain specific properties of ground and CM rotary NiTi files, their failure mechanisms and consider important factors that play a role in file failure, in particular, cyclic fatigue failure.

Having established an understanding of rotary NiTi cyclic fatigue failure, conclusions will be drawn from the information delivered in the Background and Literature Review chapters so that a research question in the form of a null hypothesis can be developed and tested. An

appropriate research methodology will be considered as a means to conduct a comparative in vitro study between HyFlexCM™ and a ground rotary NiTi instrument with an electro-polished surface: RaCe™ (FKG Dentaire, La Chaux-de-Fonds, and Switzerland). The study will compare the number of rotations to failure ( $N_f$ ), under strict conditions. The validity of the study, both internal and external, will be enhanced through a rigorous research method, the rationale for which will be explained in depth.

Data will be analysed using a statistical software package and presented graphically and discussed. The null hypothesis will be accepted or rejected, based on the significance level set for the statistical analysis.

The limitations and shortcomings of the study will be acknowledged and recommendations will be made that may broaden the scientific basis of cyclic fatigue in rotary NiTi files.

A thorough discussion will conclude this study. It will apply the findings to clinical endodontic practice and make recommendations for use of ground and controlled memory rotary NiTi instruments.



## 2. Background

### 2.1) Endodontic instrumentation and its goals

Mechanical preparation or shaping of the root canal is required to facilitate cleaning via access and exchange of irrigants within the canal so as to remove organic tissue and micro biota. Obturation, or filling and sealing of the prepared space is facilitated when shaping is carried out in an aim to fulfil certain goals. The ideal root canal preparation leaves the minor apical constriction as small as possible, has a continuous taper from apex to canal orifice and it is also desirable to have an apical cross section that approximates roundness and has the original canal within its boundaries (Harlan, Nicholls & Steiner 1996). These principles are illustrated in figure 1.

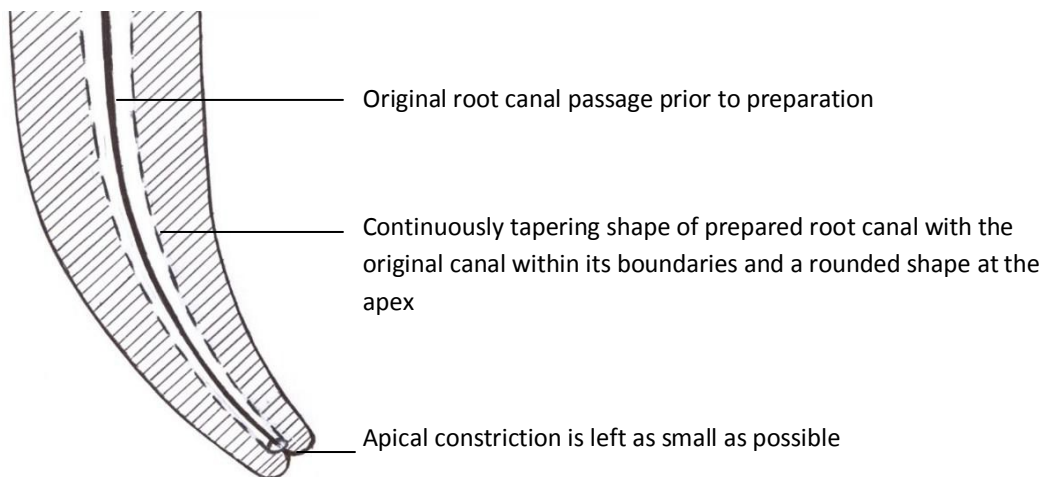


Figure 1. Root of a tooth demonstrating ideal root canal shaping goals (Author's diagram).

Complications that may occur during canal enlargement when these goals are not met include zipping, root perforation, ledging and canal transportation. These procedural mishaps occur due to straightening of the canal as it is widened (shaped) and are shown in figure 2. The instrument straightens the outer curvature of the canal. Straightening seems to

result in reduced chances of root canal success (Schafer, Schulzbongert, & Tulus, 2004). The stiffness or flexibility of the shaping instrument has a close bearing on its ability to remain centred within the canal and reduce undesirable canal preparations. Figure 3 shows how such straightening and zipping can lead to pathosis through compaction of infected dentine chips within the root.

Figure 2. Common apical preparation errors.

A, Apical zip. B, Ledge. C, Apical zip with perforation. D, Ledge with perforation (Hargreaves & Cohen, 2011).

Figure 3. A stiff endodontic file straightens the outer curvature of the canal, reducing chances of a successful outcome as contaminated dentine chips remain compacted within the root (Rhodes, 2006).

From figures 2 and 3, it clear that curved canals present the greatest risk for iatrogenic errors. However, besides straightening of the canal, instrument fracture is also a concern. Any instrument, if its ultimate strength is exceeded, or if a crack develops that propagates into the cross section of the file, such that the remaining material cannot bear the operating load, will fail (Cheung, 2009). Canal curvature also plays a significant role in failure of rotary nickel titanium files through cyclic fatigue.

Stainless steel and carbon steel have been used in both manual (hand instrumentation) and as machine driven tools. Due to the stiffness of these materials clinicians continually sought to improve their clinical techniques to limit iatrogenic mishaps associated with canal straightening and instrument fracture. Nevertheless, producing ideal canal shapes with these instruments was a laborious task. The flexibility of canal preparation instruments can be increased by altering the design features of the instruments, or by substituting stainless steel and carbon steel instruments for ones made from NiTi alloy (Schafer & Tepel, 2001). The flexibility of NiTi instruments can also be improved by altering design features or improving characteristics by heat treatment processes at manufacturing. Thermally treated instruments have been available since 2007 and the HyFlexCM™ file is the most recent of these developments (Gutmann & Gao, 2012).

Determination of instrument flexibility has been standardised in ISO standard 3630-1 as well as in the American National Standards Institute/American Dental Association Standards 28 and 58. This is done by simply bending the instrument 3mm from the tip and measuring the torque at an angle of 45 degrees (Schafer & Tepel, 2001). These standards do not seem to recognise that current heat treated NiTi instruments may be more sensitive to test temperatures above room temperatures than conventional NiTi files. This is an important fact that will later be subject to discussion.

## 2.2) NiTi flexibility

NiTi belongs to a group of metals called shape memory alloys (SMA's). Many shape memory alloys have been discovered since the mid to late 1900's but most of them are not practical for commercial applications as they contain expensive precious metals (Shaw, Churchill & Iadicola, 2008).

In the 1960's the properties of NiTi, a polycrystalline near equi-atomic SMA were discovered at the USA Naval Ordnance Laboratory and took on the acronym, NiTiNol. However, it was not until the 1990's that NiTiNol became widely used due to the unique difficulties that had to be overcome in melting and machining it in earlier years. This is due to the strong sensitivity of this alloy system to chemistry and processing (Pelton, Russell & DiCello, 2003).

NiTi is now being used in an increasing number of medical applications due to its excellent corrosion resistance, biocompatibility, shape memory characteristics and resistance to cyclic fatigue (Shaw et al., 2008).

NiTi was first investigated as manual endodontic instrument in 1988. It was found to be 2-3 times more flexible than stainless steel instruments of equivalent size (ISO N° 15); in addition it had superior resistance to fracture than stainless steel hand files (Harlan et al., 1996).

It was recognised that this material held advantages over stainless steel instruments both in terms of its potential to realise improved canal preparation shapes as well as reduce the undesirable possibility of having instruments fracture within the canal.

Figure 4. A rotary NiTi file displaying the superelastic property. On removal of the flexing force, provided it is below a certain limit, it will straighten again (Drexel, Selvaduray & Pelton, 2008).

Young's Modulus of elasticity determines the flexibility of a material. On a stress (shape) Vs strain (deformation) curve, it is the slope of the curve that is the modulus of elasticity. In figure 5, the elastic limit is the point at which the material will return to its pre-stress shape on removal of the load. After this point the material undergoes plastic deformation and is permanently deformed. The endpoint of each curve represents mechanical failure or breakage of the instrument as the ultimate tensile strength (UTS) is exceeded. The toughness of the material is represented by the area under the graph.

Figure 5. A generalised stress - strain curve for stainless steel (red line) and superelastic NiTi (black line) under tensile load (Young, Parashos & Messer, 2007).

In figure 6 below, the upper four images represent the elastic behaviour (E) of stainless steel under load by the deformation of the crystalline lattice (Hookian elasticity). The lower four images represent the superelastic NiTi that accommodates elastic deformation by transformation of crystalline phases along crystal planes.

Figure 6. At a molecular level, the superelastic property is illustrated (Stoeckel & Wu 1991).

Whereas stainless steel has an elastic limit of about 1%, superelastic NiTi can fully recover from a deformation of 8% strain (Shaw et al., 2008). Until 2010 this led to all rotary NiTi files being called superelastic. However, controlled memory (CM) files are the current exception as they have shape memory properties, described later, at room temperature.

### 2.3) Heat treatment of rotary NiTi instruments

Currently there is no accepted classification for rotary NiTi systems but for simplicity, and based on type of material used, the four groups in table 1 are representative of current systems.

Ground NiTi  1993 - present	M-Wire™ NiTi  2007 - present	R-Phase NiTi  2008 - present	Controlled Memory NiTi  2010 - present
RaCe™ System Profile™ System Protaper™ System K3™ System System GT™ Hero™ System	System GT Series X™ Profile Vortex™ System Protaper Next™ System	Twisted File™ System K3 XF™ System	HyFlexCM™ System TyphoonCM™ System 10 Series™ System

Table 1 (Authors own work). Rotary NiTi manufacturing processes with some examples of rotary file systems and the year the materials were introduced. Only the conventional ground files do not seem to benefit from some form of heat treatment (Gutmann & Gao, 2012).

Although they vary greatly in their designs, the raw NiTi wire used to manufacture ground or conventional rotary NiTi systems is very similar, if not the same (Cheung & Darvell, 2007) and consist of a near equi atomic mix of nickel and titanium. The industry standard for medical grade NiTi is called NiTiNol 508 due to it containing 50.8% Ni atoms and 49.2% Ti atoms (near equi atomic). This particular alloy is still being used in modern rotary NiTi systems such as M-Wire™ (Gutmann & Gao, 2012). Controlled memory wire has also been said to have the same composition as conventional NiTi wire (Zhou et al., 2012). However, HyFlexCM™ may be different in that it has been shown to possess a lower percentage weight of nickel than NiTiNol 508 (Testarelli et al., 2011).

It is well known that the superelastic and mechanical properties of NiTi depend on its thermo-mechanical history at manufacture (Gutmann & Gao, 2012). NiTi wire can be purchased from manufacturers in two forms: an “as drawn” form and “super elastic straight” form. The superelastic wire is softer, has a lower ultimate tensile strength (UTS) and is more ductile than the “as drawn” wire. It is technically more difficult to machine grind into NiTi files, due to excessive tool wear, than the “as drawn” wire (Zinelis, Eliades &

Eliades, 2010). A number of studies have shown that subjecting well known rotary NiTi brands to a simple heat treatment of between 350-500 °C has resulted in significantly improved properties, for example, 7% elongation (1723 MPa) to failure improves to 15% (1378 MPa) under tensile load (Zinelis, Darabara, Takase, Ogane & Papadimitriou, 2007).

Zinelis et al. (2010) stated that conventional ground files are not superelastic as this material is too soft and ductile to make an efficient cutting instrument. It seems possible that “as drawn” NiTi wire is machined into a rotary file and then has the elasticity enhanced with a heat treatment process but falling short of the full superelastic potential of the material for practical clinical reasons.

Figure 7. Stress Vs. strain curve for “as drawn” wire and wire that has been subject to different heat treatment processes (Stoeckel & Wu, 1991).

In figure 7, the heat treated wires recovers their shape better, they show less residual strain. Thus, post machining heat treatment of the wire can be used to control or “tune” the final mechanical properties (Pelton et al., 2003). The process produces a more flexible and therefore a potentially more desirable instrument for rotary NiTi use.



In figure 8, the authors noted that inspection of the HyFlexCM™ instrument revealed that heat treatment processes were performed after grinding its shape from a wire blank (Peters, Gluskin, Weiss & Han, 2012).

Figure 8. Machining grooves on a HyFlexCM™ rotary NiTi file (Peters et al., 2012)

However, the instrument in figure 8 is not a super elastic material at room temperature, it can be deformed easily and retains its shape and so has no superelastic qualities at room temperature. It will regain the pre-deformed, room temperature shape if heated above a certain temperature. This is called shape memory and is explained later.

#### 2.4) NiTi phases and characteristic temperatures

NiTi exists primarily in three forms, they are austenite, martensite (twinned martensite) and stress induced martensite (de-twinned martensite). Stress induced martensite is responsible for the superelastic effect. In addition there exists an intermediate form, the R-phase. NiTi can shift between these forms depending on the temperature of the environment and the stresses that it is subject to.

Austenite is hard and quite strong. Martensite can be easily deformed as it is ductile and soft. Stress induced martensite is highly elastic (Shen, Zhou et al., 2013). Under stress free conditions their presence and relative fractions are temperature dependant. The temperatures at which they transform are called the transformational temperatures. Bending properties are closely related to transformational temperatures (Ebihara et al., 2011).

Figure 9. Hysteresis of the martensitic transformation, it is important to note that true superelasticity (transformation of austenite to stress induced martensite) is only found in the shaded region (Stoeckel & Wu 1991).

A plot of the volume fractions (Figure 9) of austenite and martensite shows that the forward and reverse transitions do not occur at the same temperature (hysteresis). It is this hysteresis that also produces the characteristic load/unload stress-strain curve seen in the heat treated wires of figure 7, due to the material's remarkable response to both temperature and stress.

The characteristic temperatures during heating are austenite transformation start temperature ( $A_s$ ) and austenite transformation finish temperature ( $A_f$ ). There is a thermal limit to elastic deformation of stress induced martensite ( $M_d$ ), beyond this point martensite deforms like stainless steel (Stoeckel & Wu 1991). The  $M_d$  is typically 50°C above  $A_f$  (Zinelis et al., 2010).

Therefore, superelastic properties are qualities of shape memory alloys, such as NiTi, but only between  $A_f$  and  $M_d$ .

During the cooling cycle are found martensite transformation start temperature ( $M_s$ ) and martensite transformation finish temperature ( $M_f$ ). Additionally, the R-phase often occurs during cooling and before  $M_f$ , it has its own characteristic  $R_s$  and  $R_f$  (Shaw et al., 2008).

Characteristic  $A_f$  of HyflexCM™ and the four groups of rotary NiTi (for comparison) are shown in tables 2 and 3 respectively.

Due to the proprietary manufacturing processes of rotary NiTi instruments, data is not made known for the transformational temperatures or processing method. However, differential scanning calorimetry (DSC) is typically used to identify the transformational temperatures of rotary NiTi instruments. Importantly, it has been suggested that tolerances for  $A_f$  are  $\pm 5^\circ\text{C}$  using DSC (Testarelli et al., 2011). DSC is used to characterise transition temperatures in shape memory alloys by detecting changes in heat flow. However, the “bend and free recovery” test (BFR) may be a better determinant of  $A_f$  as it simulates the NiTi product in use and may be more clinically applicable. The BFR test is described later.

Heating ( $^\circ\text{C}$ )		Cooling ( $^\circ\text{C}$ )		
$A_s$	$A_f$	$M_s$	$M_f$	
Apical	$20.1 \pm 0.18$	$51.4 \pm 0.30$	$21.6 \pm 0.52$	$-30.7 \pm 1.57$
Coronal	$21.2 \pm 0.25$	$47.0 \pm 0.47$	$22.6 \pm 0.14$	$-31.9 \pm 0.13$

Table 2. Transformational temperatures for HyFlexCM™ files as determined by differential scanning calorimetry. Modified from: (Shen, Coil, Zhou, Zheng & Haapasalo, 2013).

Table 2 shows a selection of four hundred and sixty eight HyFlexCM™ instruments of different sizes at the tips as well as at the coronal end.

Table 3 shows transformational temperatures for different rotary NiTi systems, determined by differential scanning calometry. Although HyFlexCM™ is not included it was assumed by the authors (Peters et al., 2012), to have the same  $A_f$  as TyphoonCM™, however, as seen from table 2, they are quite different with HyFlexCM™ being lower for all transformational temperatures.

Table 3. Transformation temperatures for different rotary NiTi systems (Shen, Zhou et al., 2011).

## 2.5) NiTi wire manufacture

A brief description of the manufacturing processes is important as they influence the performance of the instruments.

In particular the austenite finish temperature ( $A_f$ ) is important as this dictates the completion of transition from shape memory to superelastic properties, the principles of which will be described later. The  $A_f$  can be adjusted to optimise device performance with thermo-mechanical treatment at manufacturing. The nickel content is the initial determinant of  $A_f$ , from the graph in fig. 10 it can be seen that a 1% decrease in weight of Ni can result in a nearly 100 °C reduction in  $A_f$ .

Figure 10.  $A_f$  in degrees Celsius plotted against nickel content. Near equi-atomic NiTi shape memory alloys are found along the shaded region (Pelton et al., 2003).

Impurities such as oxygen, nitrogen and carbon react strongly with titanium, thereby relatively increasing the nickel content and driving down the  $A_f$ . Impurities also negatively affect the mechanical properties as they act as stress loci where cracks can originate and propagate from in rotary NiTi files and thereby play an important role in their failure. Impurities are reduced by melting the alloy in a vacuum chamber but they cannot be completely eliminated.

However, the nickel content is a far less important in determining the  $A_f$  than the manufacturing and heat treatment process. These processes also alter other characteristics such as the hardness (Zinelis et al., 2010).

This is demonstrated in the HyflexCM™ file as the lower nickel content should result in an  $A_f$  below 0 °C, whereas may be closer to 50 °C. Therefore, the ratio of Ni:Ti is not used to characterise the alloy, but rather the transformation temperatures, and in particular  $A_f$  (Testarelli et al., 2011).

The cast ingots weigh about 2500 kg and are 50cm in diameter and need to be hot worked down to about 15cm in diameter from which the final products can be formed. Hot working is done by physically pressing, rolling and swaging at 600-900 °C. This hot working breaks up the as-cast microstructure which has little ductility, shape memory, super-elasticity or resistance to fracture (Pelton et al., 2003).

Hot working is followed by cold working processes that impart the final shape, refined microstructure, surface finish and mechanical properties. NiTi work hardens during this process i.e. it becomes harder, stronger and loses ductility as the wire is plastically deformed. To overcome this effect it must be annealed at 600-800 °C. A series of such steps or passes are required to gradually bring the material down to the final shape or diameter of “as drawn” material that is being used in ground rotary NiTi systems.

Figure 11. Basic methods for plastic deformation of shape memory alloys (Kocich, Szurman & Kurasa, 2013).

### **3. Literature Review**

A search of online databases was conducted, initially Pubmed was consulted. The search period was from 2006 and was in English. This restricted the research but did keep it current and practical.

The Pubmed open database contains abstracts of all the endodontic literature that the author has full access to via the online databases of Wiley and Sons (mainly, but not limited to International Endodontic Journal) and Science Direct (mainly, but not limited to Journal of Endodontics; Oral Surgery, Oral Medicine, Oral Pathology, Oral Radiology and Endodontology). Besides the endodontic literature; materials science and metallurgy journals occasionally publish articles pertaining to specific medical fields and a number of these were followed up on via the aforementioned databases.

The Pubmed search terms and results that they returned, followed by the number of articles that were relevant and followed up on by reviewing full text online articles in the previously mentioned journals are summarised in Table 4. Articles were followed up when relevant to nickel titanium metallurgy, manufacture, properties, fatigue testing of raw NiTi wire or rotary NiTi instruments (commercially available or prototype).



<b>Search Terms</b>	<b>Number of Results</b>	<b>Number followed up</b>
Cyclic Fatigue Rotary	81	42
Nickel Titanium Fatigue	55	10
Controlled Memory NiTi	10	3
Twisted File	24	8
M Wire NiTi	19	8

Table 4. Key search words and results (Author's own table).

Due to CM technology being introduced in 2010, it was practical to conduct a hand search of the International Endodontic Journal and the Journal of Endodontics. This was carried out from January 2010 to the present. Any paper where research had been conducted on CM rotary NiTi files was considered. This produced a further six papers that were followed up on.

Further information was gained by visiting websites of NiTi wire manufacturers. These companies supply NiTi for medical applications and have online databases of full text peer review articles, some of which have been included in the bibliography.

Websites of both of the NiTi file manufacturers used in this study were also visited ([www.coltene.com](http://www.coltene.com) and [www.fkg.com](http://www.fkg.com)).

In the search using the terms "cyclic fatigue rotary" the RaCe™ file that the author was interested in appeared many times in the number of full articles followed up on and a search for it on its own was not called for.

One systematic review was identified (Gutmann & Gao, 2012).

### 3.1) Thermo-elastic martensitic transformation

The shape memory alloys have two outstanding properties: superelasticity and the shape memory effect. The ambient temperature and the austenite finish ( $A_f$ ) temperature of the product (dictated by the specific manufacturing processes) determine which of the two properties will be predominant in the alloy.

Until the introduction of CM rotary NiTi files, all instruments displayed superelastic characteristics at and above room temperature as their  $A_f$  is around room temperature (Table 3). It should be noted that although M-wire™ has an  $A_f$  of around 50 °C, it still behaves with superelastic characteristics at room temperature. The explanation for this effect is beyond the scope of this paper. However, CM wire has strong shape memory characteristics at room temperature. Therefore an explanation of these properties is called for as they seem to strongly influence rotary NiTi performance under cyclic loading conditions.

Superelasticity refers to the recovery from a relatively large strain at a given temperature (isothermal recovery) during mechanical load - unload cycles at temperatures above  $A_f$ .

The shape memory effect is displayed by recovery of shape (strain) after a seemingly permanent deformation (stress) when NiTi is heated above  $A_f$  (Shaw et al., 2008).

Taken together this behaviour is called thermo-elastic martensitic transformation and is graphically represented in figure 12.

Figure 12. Thermo-elastic martensitic transformation (McVeigh, Vernerey, Liu & Brinson, 2006).

Austenite exists in stress free conditions and at high temperatures (above  $A_f$ ). It is a symmetric crystal cube. Ground rotary NiTi files such as RaCe™ exist entirely in this form at oral temperatures as RaCe™ has an  $A_f$  of 24.5 °C (Nakagawa, Alves, Buono & Bahia, 2013). From table 3, it can be seen that M-wire™ and CM wire also have fractions of austenite at oral temperatures.

Martensite exists either as a low temperature, low stress structure or a stress induced structure that can accommodate large strains without being permanently deformed (Shaw, 2000). Martensite is formed when austenite (temperature between  $A_s$  and  $A_f$ ) is stressed in which case it is known as detwinned or stress induced martensite (SIM). Martensite can also form under stress-free conditions when austenite is cooled below the  $M_f$ , this martensite is called twinned martensite. When twinned martensite is isothermally loaded (ambient temperature does not change) it changes shape by deforming to detwinned martensite, this is called martensitic re-orientation (MR) (Zhou et al., 2012). Detwinned martensite holds its shape when the load is removed and remains detwinned martensite unless it is heated

above  $A_f$  when it returns to austenite and regains its original shape. The shape memory property of a HyFlexCM™ rotary NiTi file is easily demonstrated in figure 13 below.



Figure 13. A HyFlexCM™ file recovers shape when placed on hand (Author's photograph).

In figure 13, a straight size 35/06 HyFlexCM™ instrument was bent 45° and maintained this shape at room temperature (left image). This happens as twinned martensite was loaded and deformed to detwinned martensite (martensite reorientation). When placed on the author's hand (right image), body temperature was sufficiently close to  $A_f$  to return the detwinned martensite to a nearly straight, and therefore a mostly austenite structure.

Therefore, as we can see from figure 13,  $A_f$  for these instruments may be much closer to body temperature than differential scanning calorimetry (DSC) results of around 50 °C suggested in table 2. It should be noted that the reliance of DSC results for practical use has been questioned and stated that the bend and free recovery test (BFR) may be a better determinant of NiTi properties for finished products (Patel, 2007).

BFR is done by bending straight twinned martensite wire into detwinned martensite and slowly heating; as the shape is recovered the "Active"  $A_f$  is determined. The temperature at full shape recovery is called the Active  $A_f$ . Active  $A_f$  for controlled memory rotary NiTi files does not seem to have been researched yet. However, Figure 13 represents a crude form of the bend and free recovery test.

Prior to the release of CM NiTi instruments the potential application of martensitic reorientation (MR) for use in rotary NiTi instruments was realised. It was explained that martensite (twinned) should be considered for use in rotary NiTi systems as it is very ductile and likely to reduce risk of fracture, however, it was noted that it is a soft material that would present clinical challenges and it would not be able to cut dentine without some form of surface hardening (Zinelis et al., 2010). It could be possible, therefore, that CM wire manufacturers have lowered the  $A_s$  and  $A_f$  to include a hard austenite fraction for improved dentine cutting at oral temperature as well as stiffen the instrument to improve torque challenge and reduce unwinding when engaging dentine. However, at oral temperatures this is likely to result in an instrument with similar characteristics to ground NiTi files, as demonstrated in figure 13, thus risk losing the benefits of martensite re-orientation.

The intermediate R-phase crystal is a rhombohedral distortion of the austenite cube and has hysteretic, reversible thermo-elastic behaviour relative to austenite as it, like martensite, can exist as a twinned or detwinned structure. However, the hysteretic difference between R-phase and austenite is very small compared to the austenite-martensite cycle, as is the strain that it can accommodate (Shaw et al., 2008). R-phase distorts at a lower force than martensite or austenite as the transformation strain is less than 10% that of martensitic re-orientation (Zhou et al., 2012).

At room temperature CM wire is composed of martensite and R-phase with small amounts of austenite (Zhou et al., 2012).

It will be touched upon later how the R-phase has been manipulated for manufacture of the Twisted File™ rotary NiTi system, however, Twisted File™ is fully austenitic at room temperature (Wu & Chung, 2012).

Figure 14. Crystalline and micro structural forms of NiTi (Shaw et al., 2008).

The earlier explanation of the thermo-elastic martensitic transformation is necessary to understand the low (favourable) elastic modulus of superelastic NiTi. Superelasticity is explained through stress induced martensite (SIM) of the austenite material at the critical stress plateau (2), as shown by the tensile stress-strain plot in figure 15.

Figure 15. Tensile stress on superelastic NiTi wire,  $A_f = 6\text{ }^\circ\text{C}$ . (1) elastic deformation of austenite; (2) plateau of martensitic transformation or SIM; (3) elastic transformation of martensite; (4) plastic deformation (Leroy, Bahia, Ehrlacher & Buono, 2012).

### 3.2) Types of Fatigue failure of rotary NiTi instruments

Failure of rotary NiTi occurs through torsional and/or cyclic loading. Although the purpose of this study is cyclic failure, it is possible that torsional fatigue plays a role and therefore requires explanation. Torsion occurs as the instrument is twisted around its axis while one end is fixed and seems to be operator dependant as it is mainly concerned with the way the instrument is manipulated within the canal.

Each time the rotating file meets resistance, for instance harder dentine or a narrow canal diameter, it is subject to torsional stress and in extreme cases when resistance is very high, the instrument may shear off (Bahia, Melo & Buono, 2008). Factors governing torque along a NiTi file include contact area between the file and the canal wall, the instrument diameter, the apical force and the preoperative canal volume (Braga et al., 2013).

Figure 16. Unwinding of a rotary NiTi file due to torque overload. A, Instrument prior to use. B, arrows show where the instrument has unwound and been permanently deformed, but not yet sheared off, the elastic limit has been exceeded (Hargreaves & Cohen, 2011).

Cyclic loading occurs as the instrument is used in a curved canal; it undergoes continuous cycles of tension (outer aspect of file) and compression (inner part of file) as it rotates around the curve.

Figure 17. Graphic representation of compression and tension in a cylindrical wire as it rotates around a curve (Patel, 2007).

The difference in strain from compression (negative value) to tension (positive value) is the strain range. The strain amplitude is half of the strain range.

Rotary NiTi files use is classified as low cycle (200-2000 RPM) but high strain amplitude (>2.5%) and can be up to 15%. This has resulted in the short fatigue life seen in these instruments (Young & Van Vliet, 2005).

Cyclic failure is an ultimate consequence of rotating a file around a curve. It is the result of repetitive stresses much lower than those that would cause failure on a single load application (Jamleh, Kobayashi, Yayata, Ebihara & Suda, 2012). A mean number of rotations will ultimately lead to file separation (Gutmann & Gao, 2012). It is cumulative and has been



identified as the leading cause of instrument separation (Larsen, Watanabe, Glickman & He, 2009).

However, there is some disagreement on this matter as some authors believe torque overload to be a more common form of failure (Braga et al., 2013). Furthermore, it seems that increasing the torsion that the instrument is subject to decreases its resistance to cyclic fatigue and vice versa (Bahia et al., 2008). Despite disagreement on the most prevalent cause of instrument failure; torsional or cyclic, it is safe to assume both play an important role in instrument fatigue failure. This has led to fatigue failure to be classified as torsional, cyclic or combined (Parashos & Messer, 2006).

Unlike stainless steel instruments that unwind prior to failure, and can be discarded upon inspection, traditional rotary NiTi files often fail without warning (Lopes, Ferreira, Elias, Moreira & Siqueira, 2009). This is especially true of an instrument that has suffered cyclic fatigue as there is no macroscopic evidence of instrument damage, whereas torsional overload plastically deforms the instrument causing unwinding, straightening, reverse winding and twisting (Parashos & Messer, 2006). These effects occur when the elastic limit of the NiTi is exceeded and plastic deformation takes place due to slipping of the crystal planes. If further forces are applied, exceeding the ultimate tensile strength limit, the instrument will shear off in the canal.

### 3.3) Comparison of properties of superelastic and CM NiTi wires

Applying an understanding of shape memory alloy properties and an awareness of the availability of relative fractions (temperature dependant) of austenite, detwinned martensite and R-phase leads to an explanation of a comparative tensile stress-strain plot between superelastic wire and CM wire at different temperature shown in figure 18.

Figure 18. Comparison of tensile failure stress-strain plots of superelastic wire ( $A_f=31 \pm 3.6$  °C) with CM wire ( $A_f= 48 \pm 3.9$  °C) of .048inch (1.22mm) diameter at oral temperatures (37 °C) and at room temperature (RT) (Zhou et al., 2012).

Although the ultimate tensile strength, as well as the plastic deformation stress of the CM wire is lower than the superelastic wire (about 1000 MPa Vs about 1400 MPa) it can be strained almost 400% more before failure. This is due to the wide plastic deformation plateau of CM wire. The CM wire represents superior toughness as the area under the CM wire curves are much greater than the superelastic wires. Raising the temperature, thereby increasing the austenite fraction in CM wire also raises the critical plateau stress. However, this plateau occurs primarily through martensite reorientation (MR) rather than stress induced martensite (SIM) which is seen at higher stress levels in the superelastic wire. With  $A_f$  of the superelastic wire being closer to 37 °C than room temperature the enhanced performance at 37 °C is expected.

Figure 19. Comparison of stress-strain load-unload plot for CM and Superelastic (SE) wire of different diameter but performed only at room temperature, again 1.22 mm (48) as well as a .64mm wire (25) (Zhou et al., 2012).

Whereas the wires in figure 18 are loaded to failure, those in figure 19 are unloaded before plastic deformation is induced. The superelastic wires exhibit nearly full recovery (low residual strain of nearly 0%) but the CM wire displays limited recovery (residual strain of about 5%). Thus, CM wire is almost plastic (provided that the temperature does not increase); the limited recovery is likely due to the small austenite fraction.

#### 3.4) Behaviour of NiTi under cyclic loading

Uni-axial (forces in one direction) tensile stress-strain relationships are very predictable compared to complex cyclic stress-strain relationships for NiTi.

Low cycle, high amplitude NiTi fatigue occurs with start parameters that are found on either the stress induced martensite (SIM) or martensite re-orientation (MR) plateau. This is why failure of rotary NiTi instruments is often unexpected. It is known that more strain is obtained on the first tension part of the cycle than on the corresponding compression part. With continual cycling the NiTi becomes offset in a tensile direction, i.e. it elongates. This is

true for both austenite and thermal martensite (analogous to CM wire in that it has mixed phases at test temperature) and indicates micro-structural changes occurring within the materials (Robertson, Pelton & Ritchie, 2012).

Under constant strain (strain controlled) conditions, the hysteresis loop narrows as the stress endured increases (figure 20). These would be the circumstances encountered by rotary NiTi files in an artificial root canal that only allows a particular trajectory or shape (strain) to be allowed by the file. With increased cycling the stress increases. Under these conditions the fatigue life of thermal martensite (analogous to CM NiTi) is superior to superelastic NiTi as the stress needed for martensite reorientation is less than that needed for stress induced martensite transformation. Furthermore, cyclic hardening of the NiTi occurs that reduces the amount of material that can undergo phase transition. This occurs more rapidly in superelastic NiTi than thermo-mechanically processed NiTi (Robertson et al., 2012). Importantly, the authors noted that cyclic fatigue testing results of NiTi in the temperature range  $A_s - A_f$  are superior to those tested in the superelastic range  $A_f - M_d$ .

Figure 20. Thermal martensite (analogous to CM wire) cycling at constant strain of  $\pm 2.5\%$ . The greatest increase in associated stress occurs in the earliest cycles. As the hysteresis loop narrows, the curve becomes steeper and the material less elastic as it work hardens (Robertson et al., 2012).

### 3.5) Mechanism of cyclic fatigue failure

Finite element analysis (FEA) uses mathematical modelling to determine the location and distribution of stress in a cycling instrument with defined material properties, geometry and load conditions. FEA has confirmed that the fracture point is near the location of maximum stress and the standard deviation between the calculated and actual fracture points decreases with increased curvature (Lee et al., 2011).

The manufacturing processes whereby file shapes are ground out from wire blanks plays a very important role in initiation of crack growth. This is due to the mechanical grinding process producing areas of work hardening and brittleness at the file surface that are more prone to cracking as stresses are concentrated in these regions. The presence of inclusions or impurities in the alloy or at the surface during processing results in areas of weakness along which cracks may propagate (Parashos & Messer, 2006).

Other studies have also noted that cracks propagate along the straight lines of machine marks and that such pathways accelerate the crack propagation process. Superficial cracking is typical of brittleness, once the remaining material cannot withstand the stress imposed on it, it fails through ductile fracture morphology (Condorelli et al., 2010).

The more ductile the material, the greater its resistance to cyclic fatigue will be (Shen, Qian, Abtin, Gao & Haapasalo, 2011).

Crack propagation in austenite seems to happen via a few un-branched cracks as austenite exists in only one crystalline form. In martensite, crack propagation is via many highly branched cracks, due to the many (sixteen) martensite variants, this slows the fatigue process and lengthens fatigue life. Furthermore, stress induced martensite (SIM) tends to be

confined to a smaller volume fraction than martensite reorientation and therefore SIM is associated with higher stress concentration (Figueiredo, Modenesi & Buono, 2009).

### 3.6) Clinical and test factors that influence number of cycles to failure ( $N_f$ )

There are many factors that influence the life-span of rotary NiTi instruments during cyclic loading, they include: working speed in revolutions per second, canal angle and radius of curvature, instrument geometry, the use of irrigant, surface treatment or finish of the instrument, metallurgical characterisation of the NiTi alloy, heat treatment of the alloy, torque and autoclave history (Jamleh et al., 2012), perhaps the most important overall determinant is the flexibility of the instrument (Lee et al., 2011).

Besides the physical parameters of the instrument and the conditions it operates in, the importance of operator experience should not be underestimated (Lee, Song, Kim, Lee & Kim, 2012). Furthermore, these factors do not occur separately but all act simultaneously to lead to instrument fracture (Bhagabati, Yadav, & Talwar, 2012). Each of these factors requires a brief explanation.

The smaller the radius of curvature that the rotary NiTi file is used in, the tighter the bend that the file is made to rotate through and the earlier the failure (Inan, Aydin, & Tunca, 2007). This has been confirmed in many experiments. Although more flexible instruments will survive longer in a given curvature, increasing the canal curvature will reduce the number of rotations to failure ( $N_f$ ) for a given instrument (Lee et al., 2011).

The greater the speed of rotation, the lower the number of cycles to failure (Lopes et al., 2009). This has been corroborated in tests using wire blanks (Young & Van Vliet, 2005).

Rotational speed is typically determined by the file manufacturer and ranges from about 300-600 RPM for devices fluted along their length, but can be up to 2000 RPM for instruments fluted at the end only, such as Lightspeed™.

The geometry of the instrument determines the volume of NiTi at the point of maximum stress and it is known that the greater the volume, the greater is the effect of cyclic fatigue for a given material. However, tests using files of similar volumes and different geometric configurations have shown significant differences in  $N_f$  between Protaper™ and Mtwo™ rotary NiTi instruments. Furthermore, mathematical models have shown a close association between instrument design and cyclic fatigue resistance (Grande, Plotino, Pecci, Malagnino, & Somma, 2006). Strain amplitude is proportional to instrument diameter, so narrower instruments are less strained. It is also possible that due to more mechanical processing than larger instruments, inclusions from the manufacturing process in smaller rotary NiTi files are broken down more and are less able to act as stress loci.

Clinically, NiTi files may deteriorate in the presence of sodium hypochlorite, a common irrigant; this may also affect fatigue failures (Topuz, Aydin, Uzun, Inan, & Tunca, 2008). However, surrounding rotary NiTi files in a fluid has a heat sink effect, limiting heat build-up in rotating instruments and increasing  $N_f$ . Heat build-up is pronounced in stress induced martensite transformation of austenite (Shen, Qian et al. 2011).

Whereas standards have been set to test for torsional strength and flexibility of stainless steel instruments, no standards currently exist to test cyclic fatigue resistance of rotary NiTi instruments (Plotino, Grande, Cordaro, Testarelli, & Gambarini, 2009)

As cyclic fatigue testing of rotary NiTi files has not been standardised, the literature has a number of widely varying methods to rotate files around a curvature until failure. These

range from steel tubes of varying radii of curvature and angles of curvature to three pin bending tests and inclined plane set-ups (figure 21). It would appear that there is a need to standardise testing protocols as it has been shown that some files behave differently to other files with different bending properties in the same artificial canal, unless the test canal is constructed to the dimensions of the files being tested (Plotino, Grande, Mazza, Petrovic, & Gambarini, 2010).

A. Three pin bending test                      B. Hollow steel tube                      C. Incline plane

Figure 21. Examples of devices that do not restrict instruments with different bending properties to the same test trajectory (Plotino et al., 2009).

For purposes of validity, it would seem reasonable to have all tested instruments perform at similar strain amplitudes. This can only be achieved when the shape of the artificial canal corresponds closely to the shape of the files being tested (strain controlled) as in figure 22.

Figure 22. A good agreement between artificial canal shape and file shape (Plotino, Grande, Melo et al., 2010).



### 3.7) Rotary NiTi surface improvements to reduce cyclic fatigue failure

There are some manufacturers that use a proprietary surface electro-polishing process to help eliminate the surface irregularities after machining the file as these areas can be the site or origin of crack propagation and fracture.

Electro polishing smoothes the surface, leaving a passive surface free of machining grooves that can induced residual stresses (Boessler, Paque, & Peters, 2009). Furthermore, crack propagation is attenuated as the cracks have to follow a tortuous pathway, they do not travel in straight lines along machine grooves and the process is therefore slowed down (Condorelli et al., 2010). An example of such an instrument is the RaCe™ file (FKG Dentaire, Switzerland) and performed significantly better in rotational fatigue tests than when it was not electro polished (Anderson, Price, & Parashos, 2007). These findings have been corroborated in other papers (Lopes, Elias, Vieira, Moreira, Marques, de Oliveira et al., 2010) and (Condorelli et al., 2010). These files do not show complete lack of surface defects however (Parashos & Messer, 2006).

In a study conducted using extracted teeth, electro polishing was found not to have any beneficial effect on cyclic fatigue tests but this is most likely due to such tests being non standardised and thereby introducing variables that could not be accounted for (Anderson et al., 2007). It has been observed that electro polishing results in increased torque during use due to electro polishing dulling the cutting blades (Boessler et al., 2009). It is the author's opinion that this may be a reason for the poorer performance ex vivo than in artificial canal tests as the rounded cutting edge is akin to a narrow landed blade and result in increased torque due to increased contact area with the canal walls.

Another way to eliminate surface defects in NiTi files is to avoid surface grinding and rather twist the blank wire into the final fluted shape. This is the method used to produce standardised stainless steel hand K files. In 2008 (SybronEndo, Orange, CA, USA) released Twisted File™ (TF™) (Bhagabati et al. 2012). According to the manufacturer it is made by transforming a super elastic NiTi wire into the R-phase by using a thermal process. In the R-phase the wire blank is twisted along its axis in conjunction with repeated heat treatment. After further thermal processes to shape set the instrument, it is converted back into the superelastic austenite form. According to a number of studies the increased flexibility of TF™ has allowed improved resistance to cyclic fatigue (Braga et al., 2013). TF™ has performed significantly better than RaCe™ in cyclic fatigue studies that the author could find (Rodrigues et al., 2011). The authors of this paper used sample sizes of 22 files for each manufacturer and explained that TF™, being more flexible than RaCe™ may be the reason for its superior performance. Unlike many similar studies, the authors also explained that the artificial canal used to perform the tests was wider than the files tested, allowing the more flexible TF™ to follow the curvature more gently therefore preventing the concentration of forces in one area that may have lead to earlier failure of the RaCe™ file.

One of the papers sourced that produced results in favour of TF™ over RaCe™ had sample sizes of two files per manufacturer (Kim, Yum, Hur, & Cheung, 2010). It was surprising that generalisations were drawn from such small sample sizes.

In general it seems that TF™ has outperformed ground files in fatigue tests (Larsen et al., 2009) and RaCe™ has outperformed non electro-polished ground instruments.

### 3.8) Thermal modification of rotary NiTi files to increase flexibility

Many design enhancements have been aimed at limiting torque failure of tapered rotary NiTi files due to so-called taper locking or screwing into the canal. These macroscopic design features include variable helical pitch angles of the cutting blades, variable rather than constant tapers, alternating cutting edges and more recently, off axis instruments. Radial lands are reduced or absent on many modern rotary NiTi instruments.

This has resulted in instruments with improved cutting efficiency, less frictional contact with the canal wall, increased flute volume for efficient debris removal and greater flexibility through reduced cross sectional areas. Whilst these changes have indirectly favoured a shift towards more flexible instruments, their flexibility was limited by the material of construction, i.e. austenite at room temperature.

It is well known that heat treatment of NiTi can enhance or eliminate the superelastic effect. Elimination generally results in a material with higher phase transition temperatures (Shen, Zhou et al., 2011), as seen in Table 3.

The raw materials used in all rotary NiTi systems have remained more or less unchanged since their introduction in 1993 (Nitinol 508). As previously mentioned the so-called second generation of instruments started in 2007 with thermo-mechanically treated M-wire™ and was followed in 2008 by TF™ (Bhagabati et al., 2012). Nevertheless, these enhanced materials are still superelastic at oral temperatures. It was postulated in 2010 that the time had arrived to consider a shape memory alloy (twinned martensitic NiTi) as an alternative material (Zinelis et al., 2010).

Since 2010 controlled memory wire has been used in a number of products, this material displays shape memory behaviour at room temperature, rather than superelasticity.

Like other ground rotary NiTi instruments, RaCe™ instruments do not seem to benefit from heat treatment processes at manufacture to improve their cyclic fatigue performance. This has been shown by significantly increased cyclic fatigue resistance of RaCe™ files after they had been exposed to heat treatment of between 350-500°C. The explanation for the results was R phase and martensite precipitation in the heat treated wire (Condorelli et al., 2010), similar therefore to CM NiTi. It is unclear why manufacturers do not supply instruments in this state, but it is likely that they lack hardness and are too ductile for clinical dentine cutting.

A similar study exposing ten K3™ instruments to post manufacture heat treatment, resulted in improved cyclic fatigue resistance and flexibility (doubled). This study was in association with Sybronendo™ and the proprietary treatment used was not disclosed (Gambarini et al., 2011). The testing temperature was not made known. The artificial canal had a 60 degree angle and 5mm radius of curvature. However, the study mentioned the thermal treatment increased the martensitic component which hints at a shape memory product, again, similar therefore to CM NiTi. Nevertheless, it cannot be assumed the process created more of a shape memory material, for instance M-wire™ has a high proportion of “micro twinned” martensite and a high  $A_f$  (but unlike CM wire, a low  $A_s$ ), yet it is a super elastic wire (Shen, Zhou et al., 2011).

### 3.9) Cyclic fatigue tests on CM wires to-date

The performance of rotary NiTi instruments in terms of number of rotations to failure ( $N_f$ ) seems to depend on their tip size and taper, design, thermo-mechanical treatment history, test temperature, test medium (air or fluid), rotation speed (RPM) and trajectory followed by the instrument in the artificial canal.

The literature revealed two papers that have compared cyclic fatigue failure of marketed controlled memory rotary NiTi files against ground files. In order to evaluate the results and seek possible methods to enhance the validity of such studies, the outstanding features of these studies are reviewed and critiqued.

The first paper (Shen, Qian et al. 2011) had a small sample size of twelve 25/04 files per group and groups were tested at two different angles. The instruments were tested at  $23 \pm 2$  °C, thus favouring the performance of the CM instruments. Rotational speed: 300RPM. The tests were done in air, an insulator that may disadvantage ground files due to rapid heat build up. A three pin bending test was used at angles of 35 and 45 degrees with 8mm radius of curvature, possibly allowing a more gentle curvature to be followed by the CM instruments. On the positive side, instruments of the same morphology were compared (Typhoon™ and TyphoonCM™). The results showed increased  $N_f$  for CM files of 300-800% over ground files.

The second paper (Shen, Qian, Abtin, Gao & Haapasalo, 2012) tested two CM file brands and three ground file brands, size 25/04 for  $N_f$  in various aqueous media against their performance in air alone. Sample size was again twelve instruments per group.

Temperature was  $23 \pm 2$  °C, rotational speed was 300 RPM in a three pin bending test with an angle of 35 degrees and 8mm radius of curvature. Instruments had the same design. The

results showed a 400-900% increased  $N_f$  for CM instruments over ground files across all media. There was no difference in  $N_f$  for ground files in air or fluid media. There was a significant ( $p < .05$ ) difference in  $N_f$ , favouring CM instrument performance in aqueous media. The authors postulated that ground files failed before heat accumulation when in air, so they performed no better when in the heat sink environment of an aqueous surrounding. Critique of this paper is similar to the first paper. Furthermore, the relatively gentle test conditions (35 degree angle at 8mm radius of curvature) may be insufficient working conditions for rapid heat build-up in the austenite instruments. Increasing the RPM may further have led to earlier failure of ground files in air.

## 4. Research Design

### 4.1) Theoretical basis

Figure 23. A Scientific method flowchart (Arsham, 1994).

It is common for engineers to study materials performance using theoretical models, however theoretical modelling of NiTi alloys using conventional theories is difficult due to the non-linear nature of superelastic phase transformations (Figueiredo, 2009). Therefore physical tests or scientific experiments are required to evaluate performance.

Such experiments aim to gather data using quantitative measures through an observational experiment that is value free and objective. The scientific approach is shown in figure 23.

From the literature that has been presented, a hypothetical generalisation regarding the superiority in terms of number of rotations to failure ( $N_f$ ) of the new controlled memory rotary NiTi files over ground files may be inferred. Empirical or scientific evidence will be

gathered through an experiment in order to demonstrate a clear relationship between NiTi material and cyclic performance.

Aspects that are critical to the scientific method are the concepts of validity and reliability.

The author will elucidate attempts at achieving these ideals by drawing on information presented in the literature and applying them to the research method.

Reproducibility of experimental methods is fundamental to the scientific approach. It will be seen that this experiment can be easily reproduced by presenting the method in detail.

Data received from the senses, in this case a visual experiment, and mathematically analysed are characteristics typical of, although not exclusive to, a positivist approach or research paradigm. Supporters of this research method view it as the only true road to gain knowledge. However, all knowledge produced by research is subjective, interpreted, political and, in part ideologically driven (Broome & Willis, 2007).

#### 4.2) Hypothesis testing

Both electro-polished ground RaCe™ files and CM files seem to be superior to non electro-polished ground files in cyclic fatigue tests.

As no direct comparison has been done between CM files (HyFlexCM™ or any others) and RaCe™ for rotational fatigue, and as the published  $A_f$  for CM instruments is well above oral temperature, this research study will test the non directional null hypothesis ( $H_0$ ): There is no difference in the number of rotations to failure for HyFlex™ and RaCe™ files. The level of significance ( $\alpha$ ) will be set at .05 ( $p < .05$ ). In order to reject the null hypothesis, a p value lower than the significance level would need to be demonstrated and the alternative



hypothesis ( $H_1$ ) would be accepted: There is a difference in number of rotations to failure for HyFlexCM™ and RaCe™ files.

The meaning of the .05 level is that we can have about a 95% confidence that the results reflect something more than random variability, i.e. a real difference between the instruments rather than chance coincidence, sampling error or the luck of the draw. The null hypothesis is the logical opposite of whatever hypothesis it is that the investigator is seeking to examine.

The .05 level of significance is conventional in many studies in the endodontic literature. The significance level of a statistical hypothesis test is the fixed probability of incorrectly rejecting the null hypothesis when it is in fact true, therefore committing a type I error. Type II error occurs when the null hypothesis is accepted when it is false.

The ability to reject the null is called power and increases when it is easy to reject the null. It increases with parametric statistics, decrease in variance, increase in samples sizes and liberal probability levels.

#### 4.3) Validity

Many studies of low cycle fatigue of NiTi have been made in the field of materials engineering as well as the endodontic literature. However these two communities approach their studies from different viewpoints. Materials engineering studies are conducted on smooth wires with constant diameters, for which strain amplitudes are easily calculated and confounding can easily be minimised.

Endodontic studies attempt to consider operating conditions similar to the clinical setting and typically compare number of rotations to failure ( $N_f$ ) for instruments from different

manufacturers. Operating parameters are not reported in terms of strain but rather as a function of angle and radius of curvature that the tests were performed under (Young & Van Vliet, 2005). A clinical setting is simulated and an attempt is made to evaluate superiority of one instrument over others under strict conditions in order to acquire relevant information that may be of benefit to clinical decision making. However, it is important to recognise that confounds cannot be eliminated in cyclic fatigue testing due to inherent differences in rotary NiTi design, flexibility, hardness, NiTi transitional temperatures, surface finish and recommended rotational speed.

Acknowledging these confounds may help to explain the outcome or test result. This is how new knowledge may be acquired.

In this experiment, the files chosen for comparison as well as the experimental method used were aimed at limiting confounding and strengthening the internal validity of the experiment. However, as the internal validity is strengthened the research can become less like the conditions of clinical use and therefore the external validity of the research may weaken. As far as possible, confounding factors will be reduced without losing sight of the goal of simulating a clinical setting.

Confounds have been categorised as instrument related or test conditions related.

#### 4.3.1) Instrument related confounds

In this experiment it is intended to determine if the manufacturing process of the files determines the outcomes of the experiment. RaCe™ is superelastic austenite NiTi with  $A_f$  of around room temperature, and is subsequently electro-polished. HyFlexCM™ is a controlled memory NiTi with  $A_f$  of about 46 to 51 °C (see table 2). It seems likely that it is ground out from the same material as the RaCe™ file, but subsequently has undergone a heat treatment

process to produce a shape memory alloy at room temperature . As many other factors as possible that may influence the result need to be eliminated or minimised if confounding factors are to be reduced.

There are a number of instrument design factors that play a role in an instrument's ability to withstand torsional or flexural loading, the design and cross sectional shape influences its fatigue characteristic (Cheung & Darvell, 2007). Specifically, the cross sectional design of the instrument seems to be the most important factor (Zhang, Cheung, & Zheng, 2010). It has been recognised that testing files of different design is a major problem and that as far as possible, files of similar cross section should be sought when the influence of the materials are being tested for (Shen, Zhou et al., 2013). The RaCe™ file was chosen as it, like the HyFlexCM™ files are triangular in cross section (figure 24). However, without further research it should not be assumed that RaCe™ and HyFlexCM™ files have equivalent cross sections at a given points along their length as the exact geometry of the triangles is not known. However, of the ground files available to the researcher, RaCe™ seems to have a close agreement in cross section to HyFlexCM™. Due to the lack of published data on HyflexCM™ files, the author undertook his own investigation. This involved fracturing a HyFlexCM™ file and viewing it under an operating microscope at 20X magnification (Figure 24).

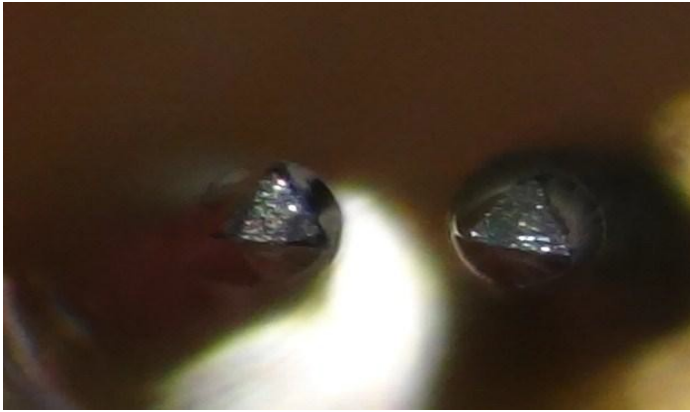


Figure 24. Fractured RaCe™ file on left and HyFlexCM™ on right, both have triangular cross sections (photographed by the author).

Of the variables governing the strains that the instruments experience under cyclic loading, it seems the volume of material under strain is the governing factor (Young & Van Vliet, 2005). The volume at a given point is a function of the tip size, taper (assuming constant tapered instruments) and cross sectional design. It was found that the larger the instrument tip size and taper is, the fewer the cycles to failure (Oh et al., 2010).

Having accounted for cross sectional design, files of equivalent tip size and taper were sought. Both file types are available in .25mm tip sizes and 6% taper over the length of the cutting blades (16mm). As instruments of this specification are commonly used in these studies, it was decided to use them. A recent paper (Braga et al., 2013) noted that sizing of some rotary NiTi files may not be as accurate as suggested by manufacturers. Therefore, a simple gauging procedure was carried out. Five of each file type were checked for agreement of file diameter along their length using a gauge (Gutta Gauge™, Dentsply, Maillefer). Both files were found to have very similar diameters at equivalent points along their length.

Despite the above precautions, macroscopically, the files are quite different. RaCe™ is a reamer with alternating cutting edges rather than a file; as such it should have fewer points

of contact with the artificial canal wall than the HyFlexCM™ file. As a result, the author believes that RaCe™ may experience less torque in an artificial canal than alternative ground files that have more cutting blade contacts. Furthermore, RaCe™ has a smooth electro-polished surface, whereas HyflexCM™ does not. This may further reduce the friction and torque.

#### 4.3.2) Test related confounds

It has been shown that small variations in the geometry of the trajectory that the files follow during testing results in significant variations in results of the tests (Plotino, Grande, Cordaro, Testarelli, & Gambarini, 2010) This is a possible reason for cyclic fatigue tests returning widely varying results and is compounded by the large scatter (non-normal distribution) of results generally found within these tests (Plotino, Grande, Mazza et al., 2010). Unless the instruments are confined to a specific trajectory, the inherent variations in flexibility of instruments due to cross sectional design and material of manufacture will allow for different trajectories to be followed and the volume of material at points of maximum strain for different instruments will vary.

Prior to the introduction of thermally enhanced NiTi systems it was acceptable to perform tests at room temperature as  $A_f$  for ground files generally are typically near room and below oral temperature (Zinelis et al., 2010). However, due to the elevated  $A_f$  of CM files, it would seem prudent to raise the test temperatures to nearer oral temperature to allow for the thermo-elastic martensitic effect that would be displayed in a clinical setting. CM files should be disadvantaged by increasing operating temperature as the harder austenite fraction will be increased.

Lubrication of the cycling instrument in the artificial canal will reduce the unfavourable effect of torque created by friction on the walls of the test apparatus. It is known that air around a NiTi instrument acts as an insulator whereas a lubricating fluid will act as a heat sink, minimising the generation and effect of heat in the instruments which is known to influence cyclic fatigue performance negatively (Young & Van Vliet, 2005). In any case, clinically, rotary NiTi files should be used in a well lubricated canal. Multipurpose oil was chosen as a lubricant for the test (3-IN-ONE®, WD-40 Company Ltd, Milton Keynes, U.K).

The test canal should be made of a material substantially harder than the cutting files or they will alter the geometry of the artificial canal and render the experiment invalid as subsequent files will follow an increasingly straight path. It is for this reason that natural teeth cannot be used in these tests. Data for the Vickers hardness (a standard test of metal hardness) of RaCe™ instruments was found to be  $415.5 \pm 15.8$  (Nakagawa et al., 2013). Data for new HyFlexCM™ files gives hardness as  $315.1 \pm 27.6$  and it increases to  $331.9 \pm 26.2$  after three clinical uses through work hardening (Shen, Coil et al., 2013). Vickers hardness of BA2 tool used for the test block steel is  $\geq 740$  (Appendix A).

Ideally, the test canal should be smooth so as to prevent surface damage to the files that may act as crack initiation sites as well as increase the friction and therefore the torque acting on the file.

Recommendations for the rotational speeds that files should be used at are set by the manufacturers and it has already been mentioned that increasing this variable has an influence on number of rotations to failure ( $N_f$ ) by reducing it. Therefore this parameter is also a potential confound. The speed that FKG Dentaire recommends for RaCe™ is 300-600 RPM (product packaging). For HyFlexCM™ it is 500 RPM (product packaging). It was decided

to eliminate this potential confound by choosing to use a rotational speed of 500 RPM for both files.

#### 4.4) Data analysis

The objective of this study is to test fatigue failure of two types of instruments. Random samples of each type of instrument (HyFlexCM™, sample size= 47 and RaCe™, sample size 48) were rotated to failure. The hypothesis to be tested is: there is no difference between the numbers of rotations to failure between the instruments. This will be tested at a .05 level of significance.

Since the data is number of rotations to failure (i.e. number of rotations until the event of failure happens), it is considered a survival data. Survival data records the number of intervals (such as time intervals or, as in this study, number of rotations to failure) that lapse before the event of interest occurs. Survival analysis is commonly used in engineering applications to compare how long components function before failing. Survival data usually deviates from a normal distribution and therefore cannot be analysed with tests of means such as t tests or ANOVA that require the data to be normally distributed. As mentioned previously, cyclic failure tests on NiTi files are non-normal in distribution. Descriptive statistics and tests of normality of the data will be presented using the histogram, boxplot and normal probability plot (Q-Q plot) to provide information on the normality of the distributions. The Cox survival analysis model will be used for testing the null hypothesis. Kaplan Meier survival plots will be used to graphically compare the data.

Pilot studies and power analysis of small sample results can be used to increase the power (to reject the null hypothesis) of the intended study by selecting an appropriate sample size. However, for the following reasons a pilot study was not conducted. Firstly, the author did not want to limit the test sample size by using some of the available files for a pilot study. Secondly, the sample sizes are much larger than those typically encountered in similar studies. Post experimental power analysis is called the objective power. This type of analysis will be commented on later.

It is not possible to fully randomise the sample with this type of experiment without ordering files of different Lot Numbers from suppliers. This approach would be impractical. Therefore files of the same Lot Number were obtained from suppliers for each file type. The files stocked by each supplier would represent the sampling frame and the delivered files do represent a randomly acquired sample.

Some studies narrow the sample down by eliminating instruments with surface defects. This approach may increase the internal validity. However, it is not clinically practical or applicable and would greatly limit the external validity so it was decided not to incorporate this step in file selection.

#### 4.5) Reliability

Because different handpieces can be set to rotate at different speeds it is important, for standardising and comparison to similar experiments, i.e. reproducibility, that results are given as number of rotations of the file until failure ( $N_f$ ).



In this experiment the only dependant variable to be measured is the time, in seconds, to failure of the instrument. It is important to get the reliability of this measure as close to 1 as possible. Reliability is the true amount divided by the amount obtained.

For practical reasons it was decided to hand time the experiment. It was decided to time the start of the file turning with a stopwatch in hundredths of seconds. This would coincide with starting the rotation of the file by pressing the footswitch on the motor. The stopwatch would be stopped on visual evidence of file failure then multiply the time and RPM of the motor to arrive at the number of rotations to failure ( $N_f$ ). Reliability would be maximised if the person starting the file rotation was also responsible for timing each file failure throughout the experiment. Thus, the author undertook this role.

The evaluation of reliability for this experiment was the human error or reaction time in starting and stopping the stopwatch. As the error is similar for all the files it can be considered to have a negligibly small effect on the statistical outcome. Many such experiments have made use of similar timing techniques.

#### 4.6) Experimental method

Fifty four HyFlexCM™ files (LOT F06603) were kindly sponsored by Coltène/Whaledent (Altstätten, Switzerland) and fifty RaCe™ files (LOT 23520) were ordered from the U.K distributor, Schottlander.

A precision engineering firm; Waveney Precision, Bungay, Norfolk, U.K, was commissioned to manufacture an artificial canal in hardened steel to specific parameters. The metal chosen for the test block was tempered BA2 tool steel with a Vickers hardness of  $\geq 740$ .

The overall length of the canal was 22mm. At the narrowest end it was 0.35mm wide and had a constant taper of 6% over the first 17mm. From 17mm to the widest end there was no taper. The widest end, therefore, was 1.37mm in diameter. A 90 degree angle of curvature with an inner radius of curvature of 5mm was placed in the canal. The curvature started 3mm from the narrow end. The depth was 2mm.

Using a CAD programme, a copper die or negative of the canal was created on a precision computer controlled milling machine. Then, using electrical discharge machining (EDM), the copper die was used to electrically etch the negative form of the die into the steel. The advantage of EDM is that very hard steels can be machined. A PDF copy of the data supplied by the engineering firm as well as the geometry of the artificial canal can be found in Appendix B.



Figure 25. The artificial canal in the steel block (photographed by the author).

A 6:1 reduction endodontic handpiece (Sirona, VDW), was used to run the files. The handpiece was powered by a torque controlled electric motor (VDW Silver) under microprocessor management from the corresponding control. The settings used were at the maximum torque of 410 N/cm and 500 RPM. The instrument was automatically calibrated prior to use. The motor was controlled by an on/off footswitch.

It was important to accurately reproduce the trajectory for all files in the canal on each insertion. To this end a jig was made to ensure spatial reproduction of the handpiece and metal test block relationship after each file exchange. It represented a simplification of the “block and rod” assembly used in similar experiments. The jig allowed for testing files of different lengths as it was found that the HyFlexCM™ files are about 1mm longer than the RaCe™ files due to different shank lengths.

Using a workbench vice, a size 6 allen key (steel tool with hexagonal cross section) was placed behind the test block with 30mm protruding above the test block and both securely fastened in the vice. A small G clamp was also used higher up the block to further improve stability of the allen key.

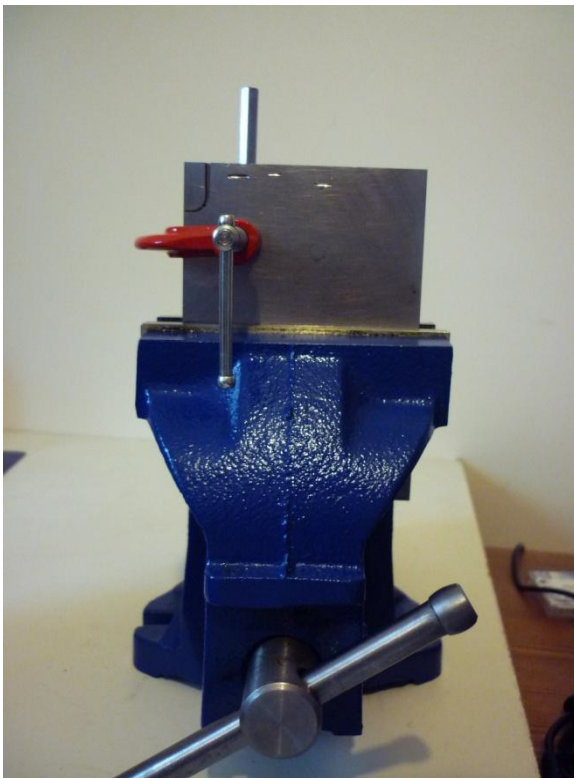


Figure 26. Vice and G clamp assembly to connect allen key to test block (photographed by the author).

A RaCe™ file was placed in the handpiece and positioned in the canal with the tip flush with the end of the canal. In a staged process the handpiece was connected to the allan key using hard bis-acrylic resin (Protemp™, 3M ESPE). The resin extended beyond the length of the allan key where it housed a 6mm nut.

Once the acrylic was fully cured the handpiece and resin jig were pulled off the allan key and trimmed. A 6mm engineering screw (vertical stop) had a locking nut screwed onto it, and then it was screwed into the nut on the top of the jig.



Fig 27. The acrylic jig secure on the handpiece. The nut in the jig accommodates the vertical stop screw (photographed by the author).



Figure 28. The full test assembly with vertical stop screw and locking nut (photographed by the author).

The hexagonal cross section of the allan key meant the jig could be re-located on it in the same position each time it was removed to replace a broken file. The stopping screw and locking bolt maintained the vertical position.

The frictional contact between the acrylic jig and the allan key was such that they did not need further fixing to each other. In fact it required regular lubrication with multipurpose oil (3-IN-ONE™) to aid removal and replacement, the required removal force was estimated at about 100 N.

This assembly was then turned through 90 degrees and clamped to a worktop. This allowed for a horizontal placement of the test block so lubricant oil could not drain from the canal while the files rotated.

A number of each file were run to failure in order to test the apparatus.

The room used for the experiment was then heated with an electric oil heater (DeLonghi, 3000 Watt). All the materials used for the experiment stayed in the room while it heated up.

The HyFlexCM™ files were labelled Group 1 and were run to failure in succession. The air temperature was recorded at every tenth file. An Oregon Scientific™, model SL103, digital air thermometer (Oregon Scientific, Tualatin, Oregon, USA) recorded the temperature. The test of the HyFlexCM™ files started with the temperature at 34.1 °C and it slowly increased, ending at 36.1 °C. The RaCe™ test temperature started at 36.1 °C and decreased slightly to 35.6 °C at the end.

The position of the files in the canal was such that the tip was flush at the end of the canal. This was verified visually using 2.5X magnification loupes with LED illumination (Keeler™), being sure to avoid parallax errors. The canal was lubricated after placement of each file with 3-IN-ONE™ oil. The rubber stop (blue rubber ring on the file in figure 28) on the tested file was positioned against the top of the block to prevent lubricant oil from being extruded from the canal due to the Archimedean screw effect created by the rotating files.

This method was reproduced for the RaCe™ files, Group 2, and they were run to failure in the same way.

Raw data (time to failure) was collected and recorded by the author. The time to failure of each file was recorded in hundredths of seconds with digital stopwatch and tabulated for each file of each group. The raw data was converted to number of rotations to failure (Nf) by multiplying by 8.333 (rotation speed was 500 RPM). This data was rounded down to the second decimal place and entered into the statistic analysis software package, SPSS™ for Windows, Version 21 (IBM). See Appendix C for data table. It is important to keep raw data

as any faults in the experiment, that may be detected subsequently can be corrected.

Inaccurate data recording would influence the validity of the experiment.

These raw data records were scanned and kept on a hard-drive as well as being stored on two portable USB drives, thus storing at different locations to prevent data loss.

#### 4.7) Limitations of the experimental method

There are numerous shortcomings to the experimental method that need to be recognised as they could be reviewed in future experiments of this kind to enhance both the internal and external validity.

##### 4.7.1) Limitations pertaining to internal validity

- 1) The standardised endodontic instrument flexibility test, as mentioned in the introduction to this dissertation could be performed and recorded at the test temperature prior to the fatigue test being performed. This may give important information on the thermo-elastic phase status of the tested files.
- 2) To better understand the behaviour of a given material, attempts to determine its Active  $A_f$  could be made. This can be as simple as bending a sample of the instruments and placing them in a bath of water and slowly increasing the temperature until they have recovered their shape. Although this method is a crude form of the bend and free recovery test, it is very accurate and has been described by materials scientists.

- 3) Using artificial canals with a range of different radii of curvature may help to build a better picture of the factors that play a role in cyclic failure. However, it is the opinion of the author that it is the position of the radius in the canal that is of greatest importance. For instance, the curvature used in this experiment started 3mm ( $D_3$ ) from the apex ( $D_0$ ) or file tip. A simple mathematical analysis (Appendix B) shows the middle of the curvature is around 7 mm from the tip. Failures were found to occur at the 7mm mark, which is not surprising. If the curvature was made to start at the terminus, the files would have broken around the 4mm mark and possibly led to different results. This is due to  $A_f$  decreasing along the file towards the shank (Table 2).
- 4) The artificial canal walls should, ideally be perfectly smooth. The method used to create the artificial canal in this experiment was the same as used by experts in this field as cited earlier. However, it was noted that this produced a surface that is not as smooth as the finish on the external surfaces of the test block. It may be possible to electro-polish the walls of the canal to eliminate these surface irregularities and therefore reduce the frictional component on the file that will have the effect of increasing the torque, heat generation and potentially scouring the surface of the files. These factors are known to reduce performance in cyclic fatigue testing and could potentially affect different rotary NiTi files to differing degrees.



### 3.7.2) Limitations pertaining to external validity

As previously noted, cyclic fatigue tests cannot be performed in teeth, so the use of an artificial canal in itself is not regarded as a shortcoming. However, some aspects of these tests must be recognised as they may enhance the validity as pertains to clinical use.

- 1) Samples of files from different LOT numbers may provide a better sampling frame for a more accurate generalisation of results to the brands as a whole. This would need to apply to all NiTi brands in the test to avoid bias. However, there are real practical difficulties in doing this. A range of LOT numbers may be acquired if the files are ordered from a number of different suppliers. However, some rotary NiTi files, including RaCe™ are only available through sole distributors in the U.K. and this likely to restrict access to a range of LOT numbers at any given time.
- 2) Data for the temperature within a root canal during clinical endodontic treatment could not be found so it was assumed to be near body temperature.
- 3) Clinically, rotary NiTi files are not held statically and allowed to rotate, but are rather used in an up and down “pecking” motion. Tests incorporating this type of movement may yield useful information.

- 4) Root canal preparation with rotary NiTi files typically involves about 3 to 6 instruments per tooth. As it is known that it is the volume of material at the greatest curvature that determines the likeliness of failure, it would be prudent to test files larger than the 25/06 files that are commonly used in cyclic fatigue tests.
  
- 5) It is possible that common irrigants used in endodontics e.g. sodium hypochlorite, EDTA, citric acid and chlorhexidine could affect cyclic fatigue performance.
  
- 6) It is possible that the effects of autoclaving rotary NiTi files during sterilization procedures could affect cyclic fatigue performance. However, it is considered good clinical practice to use new files on each case and it is regulatory in the U.K to dispose of endodontic instruments after a single use.

## 5) Results

### 5.1) Descriptive and inferential statistics

Descriptive statistics and tests of normality of the data are presented in Tables 6 and 7 below. It is clear from the descriptive statistics that the data of the two types of instruments deviates from normality. For example Table 1 shows that RaCe™ data has much higher peak than the normal distribution (based on the large kurtosis value) and is skewed to the left (based on the large negative skewness value). The opposite can be seen for HyFlexCM™ where the distribution is much flatter (as determined by the low kurtosis) and is skewed to the right (as determined by the positive skewness value). The same conclusions can be seen in the histograms (Figure 31).

Based on the Kolmogorov-Smirnov test of normality, the data of both RaCe™ and HyFlexCM™ deviate from normality ( $p < .05$  for the two devices). Shapiro-Wilk test of normality showed that the data for HyFlexCM™ clearly deviates from normality with p-value less than .05. However, for RaCe™ the test of normality of the data is marginally not significant (just above .05).

Group	N	Minimum	Maximum	Mean	Std. Deviation	Median	Kurtosis	Skewness
HyFlex	47	41.57	190.16	96.1549	34.09492	88.6600	.387	.721
RaCe	48	8.50	145.58	98.8987	23.70105	99.3700	3.909	-1.251

Table 6. Descriptive statistics of the data.

	Group	Kolmogorov-Smirnov <sup>a</sup>			Shapiro-Wilk		
		Statistic	df	Sig.	Statistic	Df	Sig.
Rotations to Failure	HyFlex	.129	47	.049	.954	47	.062
	RaCe	.136	48	.026	.916	48	.002

Table 7. Tests of normality.

The Q-Q plot can be used to graphically represent how close a continuous data set corresponds to a normal distribution. Deviation from the oblique line, as seen in both plots below, represents non-normal distributions.

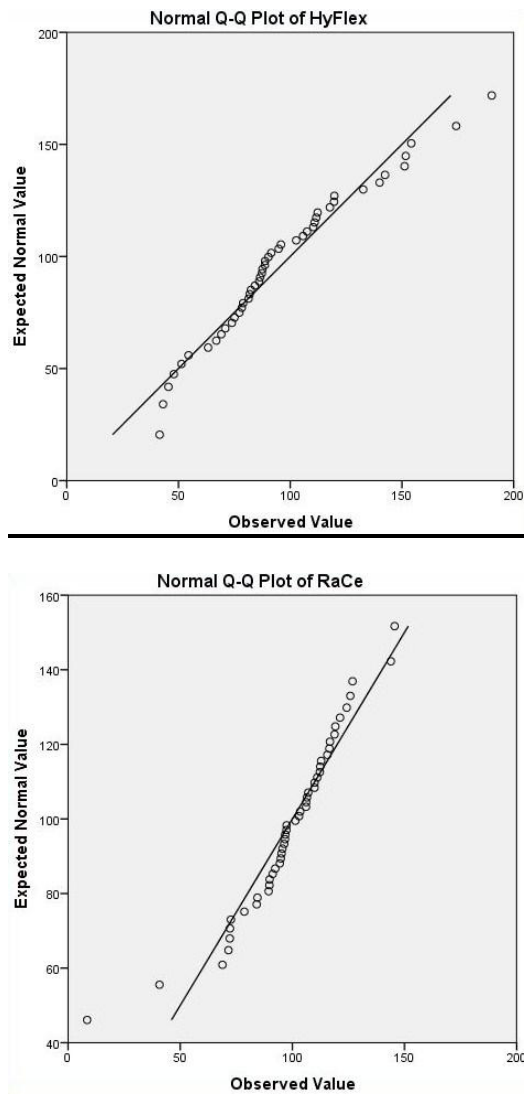


Figure 29. Q-Q plots for HyFlexCM™ and RaCe™ groups.

A boxplot breaks the data up into quartiles and can help identify differences in the dispersion and skewness of the data. The lower boundary of the box is the first quartile, the band in the middle of the box is the second quartile or median and the upper boundary is the third quartile. In SPSS™ the whiskers extend a maximum of 1.5 times the height of the

box. Outliers in both groups can be easily identified in the boxplot below; their data points, as entered in SPSS™ are represented by circles. Extreme outliers are represented with a star.

### Rotations to Failure

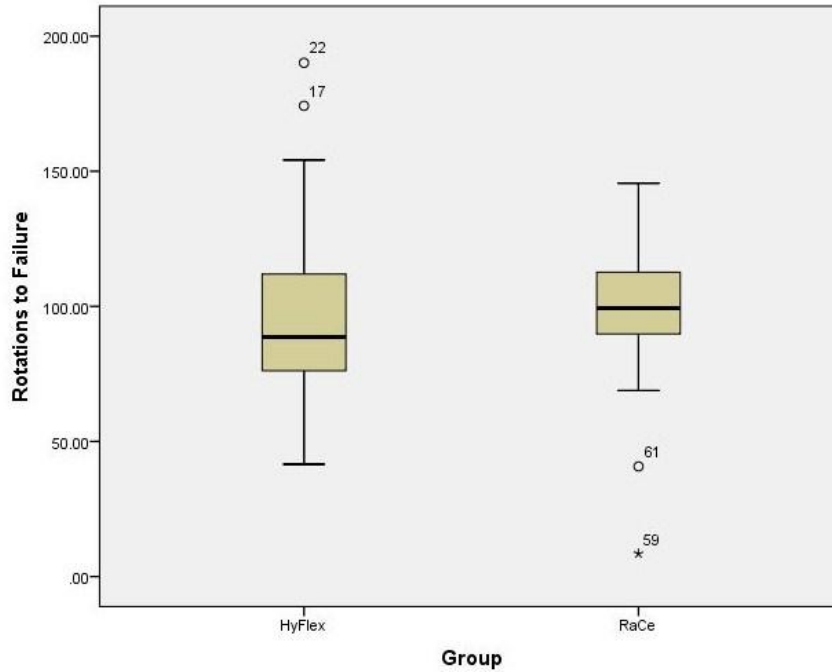


Figure 30. Box plots of  $N_f$  for each group.

Histograms can be used to evaluate the frequency of data and are a representation of the distribution of the data values. They can help to evaluate the central location, width of spread and shape of the data. SPSS™ can overlay the histogram with a normal plot.

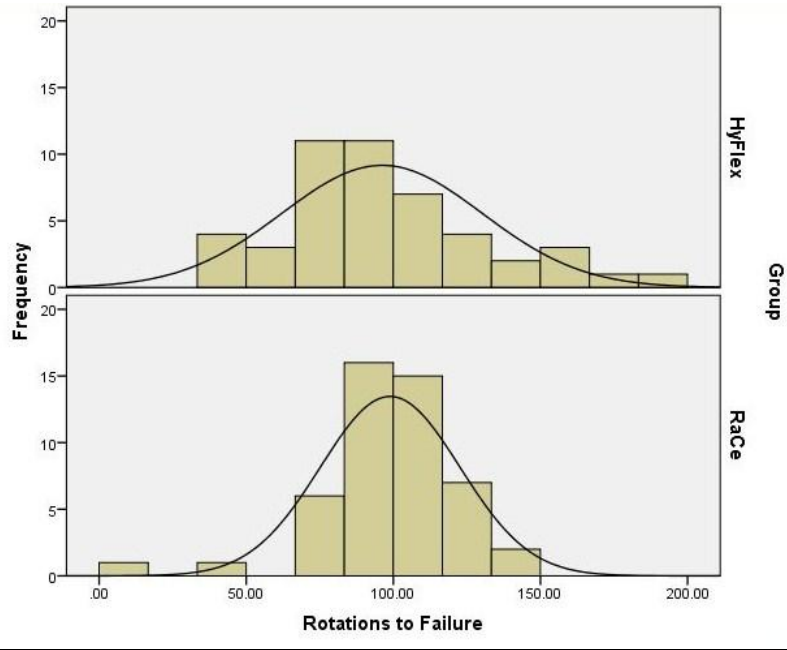


Figure. 31 Histograms overlaid with normal plots for both file groups.

Based on both descriptive and inferential statistics of tests of normality, the data is considered to deviate from normality.

## 5.2) Cox survival model results and Kaplan Meier survival plots

The data was analysed using survival analysis models. Cox survival model was used and the results are presented in Table 8. It shows that there is no significant difference in the number of rotations before failure between the two devices ( $p = .838$  which is larger than .05 level of significance). The analysis was repeated using the bootstrapping method which is more suitable if there is concern that the sample size is small (Table 9). The results remain insignificant ( $p = .847$ ).

	B	SE	Wald	df	Sig.	Exp(B)	95.0% CI for Exp(B)	
							Lower	Upper
G	.044	.216	.042	1	.838	1.045	.685	1.595

Table 8. Results of Cox survival model.

	B	Bootstrap		Sig. (2-tailed)	95% Confidence Interval	
		Bias	Std. Error		Lower	Upper
G	.044	-.017	.215	.847	-.390	.458

Table 9. Results of Cox survival model using bootstrapping.

A survival plot using a Kaplan-Meier survival curve was plotted for the number of rotations before failure by instrument type (Figure 32). The survival curve shows some interesting patterns of number of rotations before failure for the two instruments. It shows that the survival rate (probability of no failure) was lower for HyFlexCM™ than RaCe™ at early number of rotations (in other words HyFlexCM™ tend to fail more than RaCe™ at low number of rotations). The opposite happens at higher number of rotations where HyFlexCM™ shows a higher survival rate at higher number of rotations. In other words, once HyFlexCM™ passes about 110 rotations, its performance becomes better than RaCe™.

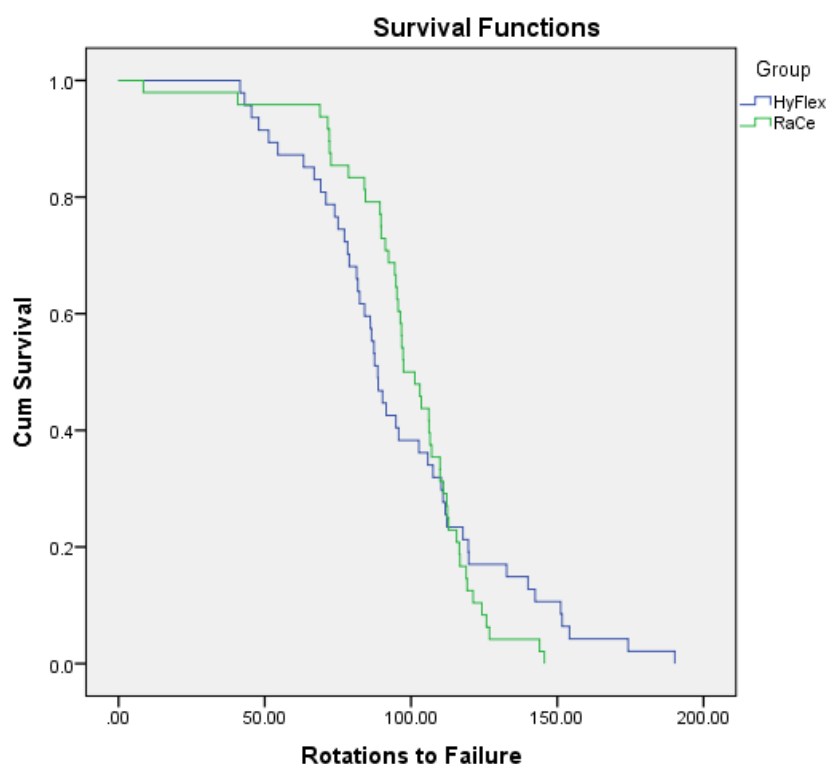


Figure 32. Kaplan-Meier survival curve of number of rations before failure.

To investigate this pattern further, survival analysis was repeated two times; once for data with rotation that less than 110 and the other for rotation more or equal to 110. The results for the first analysis are presented in Tables 10 and 11 and Figure 33. The results for the second analysis are presented in Tables 12 and 13 and Figure 34.

The results of survival analysis at low number of rotations shows that there is a high significant difference between the two instruments ( $p = .002 < .05$ ). The same conclusion can be reached using bootstrapping as shown in Table 6 ( $p = .003 < .05$ ). Figure 4 of Kaplan-Meir



survival curves clearly shows that HyFlexCM™ is inferior compared with RaCe™ at lower number of rotations.

-2 Log Likelihood	Overall (score)			Change From Previous Step			Change From Previous Block		
	Chi-square	df	Sig.	Chi-square	df	Sig.	Chi-square	df	Sig.
409.733	9.500	1	.002	8.952	1	.003	8.952	1	.003

Table 10. Results of Cox survival model for low rotations (less than 110).

	B	SE	Wald	df	Sig.	Exp(B)	95.0% CI for Exp(B)	
							Lower	Upper
G	-.785	.260	9.104	1	.003	.456	.274	.759

Table 11. Results of Cox survival model using bootstrapping for low rotations (less than 110).

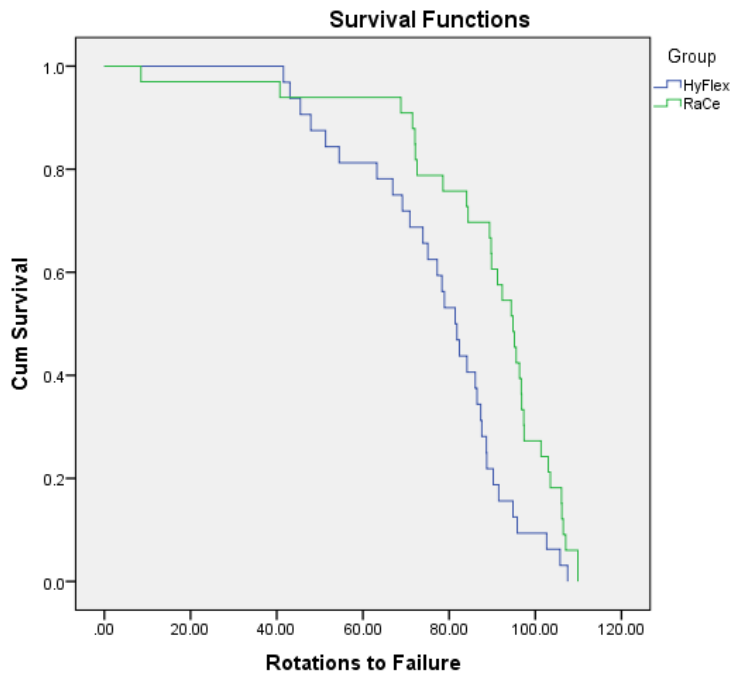


Figure 33. Kaplan-Meier survival curve of at low number of rotations (less than 110).

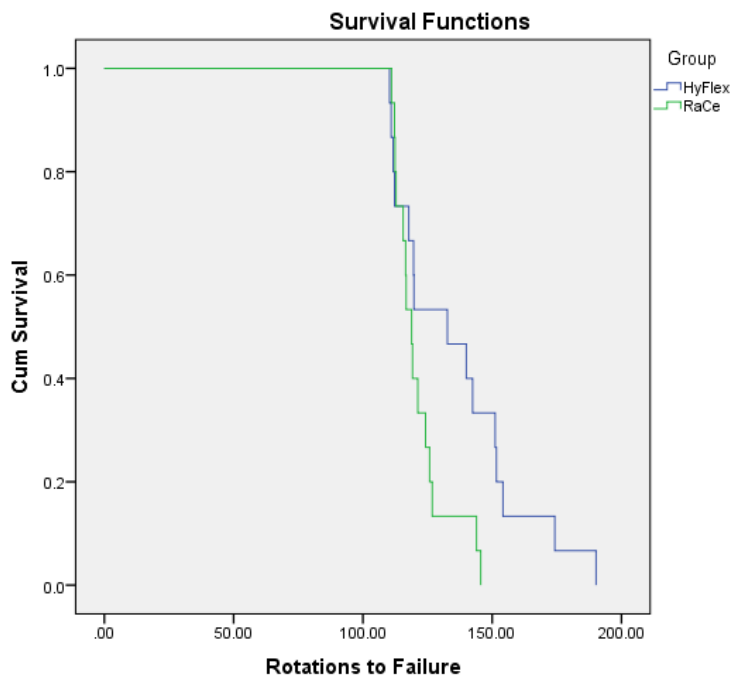


Figure 34. Kaplan-Meier survival curve at high number of rotations (110 and higher).

The results of survival analysis at high number of rotations (110 and higher) shows that there is no significant difference between the two devices but the p value was just at the margin of significance threshold ( $p = .051 > .05$ ). However, using bootstrapping which is more suitable

in these cases of lower sample size, shows a significant difference ( $p = .039 < .05$ ). Figure 34 of Kaplan-Meir survival curves clearly shows that HyFlexCM™ performs better at higher rotations compared with RaCe™.

	B	SE	Wald	df	Sig.	Exp(B)	95.0% CI for Exp(B)	
							Lower	Upper
G	.822	.422	3.795	1	.051	2.274	.995	5.199

Table 12. Results of Cox survival model for high rotations (110 and more).

	B	Bootstrap <sup>a</sup>		Sig. (2-tailed)	95% Confidence Interval	
		Bias	Std. Error		Lower	Upper

a. Unless otherwise noted, bootstrap results are based on 1000 bootstrap samples

Table 13. Results of Cox survival model using bootstrapping for high rotations (110 and more).

### 5.3) Objective power

Rejection of the null has failed so there is a danger of committing a type II error (failing to reject a false null). The power of a hypothesis test is 1 minus the probability of a type II error. However there does not seem to be any need to calculate this post hoc, as by definition, the design of the experiment is such that it has a low ability to detect a difference between the two groups. It is most likely that the ability to detect a difference in the groups of a specific size lies within the science of the experiment. Specifically, decreasing the test temperature to a specific level.

#### 5.4) Discussion of results

Both groups had outliers. HyFlexCM™ had upper limit outliers whereas RaCe™ had lower limit outliers. Due to the outliers the number of rotations to failure ( $N_f$ ) range is very similar for both groups but there is a greater spread for the HyFlexCM™ group. The most obvious outlier is the early RaCe™ failure after 8.33 rotations. In one way, HyFlexCM™ performed better in that they had a greater frequency of better performing instruments than RaCe™. However, besides the RaCe™ early failure, HyFlexCM™ also performed worse at the lower end of the  $N_f$  range.

The mean scores for both groups are very similar.

Within the limitations of this study, these findings do not support the superior cyclic fatigue reports for CM rotary NiTi files discussed in earlier studies.

The possible reasons for this are that the test temperature reduced the protective martensitic fraction in the instruments. Furthermore, studies have shown that the  $A_f$  of these instruments is lower towards the shank than the apical region, possibly due to the heat treatment process being more effective at the narrower tip (Shen, Coil et al., 2013). It was observed that most of the instruments failed around 7mm from the tip this test. It is likely that the  $A_f$  of HyFlexCM™ wire may not be as high as studies using differential scanning calorimetry (DSC) have shown.

Nevertheless, HyFlexCM™ did perform well beyond 110 rotations. The reason for their poor lower rotation results may be their lack of a protective electro-polished surface that the RaCe™ instruments benefit from. The protective RaCe™ surface may become worn at about 110 rotations after which the small martensitic fraction in the HyFlexCM™ file is

advantageous. The early RaCe™ failure is likely from due to an inclusion during the manufacturing process as it is not likely to be a defect from surface machining.

## 6) Conclusion

The enhanced flexibility of superelastic or austenitic NiTi has been cited as the reason for the rotary NiTi revolution in endodontics. However, CM products are attempting to make use of the shape memory qualities, rather than the superelastic qualities of the nickel titanium shape memory alloy system.

The new generation of CM Wire, R-Phase and M- wire™ products are likely to reduce procedural errors such as ledging and transportation (Gambarini et al., 2011). Their increased flexibility should reduce cyclic fatigue failure as well. The astute clinician, will, or should be aware of the relative advantages and disadvantages of the materials currently available in the preparation or shaping of a root canal space.

Until recently, the products available to the endodontic armamentarium seem to have been made of stable austenitic NiTi or a product with an  $A_f$  of around room temperature.

However, the properties of this material, through simple heat treatment manipulation allow the flexibility to be greatly increased by raising the transformation temperatures and in particular, the  $A_f$ . This is seen in both M-wire™ as well as CM products; however M-wire™ incorporates a mechanical process as well as heat treatment and has strong superelastic characteristics, even at room temperature.

The increased flexibility of TF™ has not resulted in increased  $A_f$ , but this is more through manipulation of R phase NiTi than re-working of stable austenite.

Increasing the  $A_f$  temperature above operating temperatures seems to increase the martensitic and possibly the R-phase components and lead to a more flexible material with the possibility for improved preparation shapes, through reduced potential for straightening and reducing failures through cyclic fatigue. CM material will, or should, behave as a shape memory alloy rather than a superelastic alloy when operating at around oral temperatures. These temperatures are yet to be determined, but hold the key to transparent testing and evaluation of instruments against competitors.

Despite the obvious advantages to using ductile shape memory, rather than superelastic NiTi alloys, their use is not without disadvantage. The “torquability” of a rotary NiTi instrument is a term used to indicate its ability to deliver the torque applied at the shank, through the instrument, to the apical extent without distortion of the instrument. Herein lies the disadvantage of CM alloys, in other words, they are more likely to unwind as they are more plastic, or malleable. The result is that the cutting efficiency is decreased. As the cutting blade edge becomes aligned with the long axis of the canal, the ability to auger debris from the canal is lost. However, unwinding will protect against torque fatigue failure and therefore may benefit the more inexperienced operator.

Unwinding may be countered by decreasing the torque of the handpiece and accommodating it with an increase in RPM. More cynically, this effect can be countered with a decrease in  $A_f$ . This would present a material that has the attractive benefits of a shape memory alloy when examined at room temperature yet behave more like a superelastic material, with the benefits of superelastic torquability and reduced unwinding in clinical use. Of course, it is likely that exact manipulation or tuning of NiTi transformation temperatures to high tolerances is technically very challenging and has not yet been mastered. This is quite

likely to be made more difficult in rotary NiTi products that vary in their cross sectional shape, size and taper.

It has been stated that differential scanning calorimetry should not be used to determine  $A_f$  for clinical applications, but rather the “bend and free recovery” (BFR) test (Patel 2007). In these tests a bent instrument is carefully heated and its transformational temperatures are determined by straightening while heated. In orthodontic wires these tests have shown  $A_f$  to be significantly lower than figures given by manufacturers (Obaisi et al., 2013). As stated earlier, the  $A_f$  determined by the BFR test is given as Active  $A_f$ . There may be a very narrow temperature range that the  $A_f$  or Active  $A_f$  equivalent would need to lie within to take advantage of martensite, R-phase and austenite in clinically beneficial ratios.

Standardising rotary NiTi cyclic fatigue testing presents a great challenge due to confounding factors. It may never be possible to confidently compare the performance of one instrument to another. This is made more difficult with instruments of variable taper and the advent of offset files such as Protaper Next™. However, there are many ways that confounds can be reduced and they have been discussed at length. Certainly, one of the most important acknowledgments should be to perform the tests at oral temperature. This is especially true when instrument manufacturers claim to have superior performance from a product with an  $A_f$  above body temperature or even room temperature.

Standardising authorities need to appreciate the relevance of testing instrument flexibility of NiTi instruments with elevated  $A_f$  at clinically relevant temperatures as there seems to be a close relationship between the flexibility and cyclic fatigue failure.

## **7) Recommendations**

The application of controlled memory rotary NiTi instruments may need to be restricted to instruments of a larger tip size. This is because the torquability will likely increase for CM files with an increase in tip size simply through an increase in volume of the material being torqued. A clinical study has shown that smaller HyFlexCM™ NiTi files unwind more than larger instruments (Shen, Coil et al., 2013). Use of such larger instruments would fulfil biological principles of root canal shaping; this is especially true for infected or necrotic canals.

This approach facilitates irrigant access to the apical zone as well as access to the apical zone for mechanical, sonic or passive ultrasonic “activation” of the irrigant. Use of CM NiTi may limit the risks associated with straightening such canal preparations. It is well known that the apical 3mm of root canals are the most likely area for canal ramifications, i.e. the apical delta (Rhodes, 2006).

There are, however, other arguments for larger apical preparations such as improved access for placement of antiseptic root canal dressing materials and facilitation of obturation by machining the oval shaped root canal into a rounder shape to accommodate gutta percha cones.

However, preparation of an already naturally wide root canal is not necessary as irrigant access is already facilitated and obturation with gutta percha (normally requiring an apical stop) is not required as products such as MTA may be better alternatives in such cases.

It must be appreciated that rotary NiTi preparations may be enhanced by embracing the full range of NiTi technology available to today’s clinician. By hybridising rotary NiTi canal preparation, the benefits of particular instruments can be taken advantage of throughout



canal preparation. For instance, straightening of the root canal in the coronal portion, coronal flaring, is a prerequisite for biological root canal shaping goals. It would be most sensible to use an austenite material in this zone. For reasons already explained, smaller size superelastic NiTi files are not likely to fail due to cyclic fatigue. Therefore they may be used in glide-path preparation and a perhaps a little larger. Further preparation and apical enlargement may be completed with a more flexible heat treated product such as M-wire™, TF™ or a CM product.

As previously mentioned, the primary factor implicated in rotary NiTi failure is operator experience. It is likely that other iatrogenic errors associated with canal straightening are closely linked to practitioner experience as well. Although newer rotary NiTi instruments may reduce the chances for mishaps, understanding their limitations and their proper use is of utmost importance. Nevertheless, severely curved canals present a challenge, even to the very experienced clinician. CM type instruments may reduce procedural errors and instrument failure in such canals, provided the preparation size is gradually increased using many instruments. The technique is described in the HyFlexCM™ product packaging and may limit instrument unwinding.

As with all rotary NiTi instruments, fundamental principles should be adhered to when using CM files to limit risk of cyclic fatigue failure. These include complying with manufacturer's guidelines, using only new instruments in well lubricated canals, not allowing the file to rotate while held in a static position, maintaining patency and cleaning of dentine debris from the file flutes after each insertion.

## References

- Anderson, M. E., Price, J. W., & Parashos, P. (2007). Fracture resistance of electropolished rotary nickel-titanium endodontic instruments. *Journal of Endodontics*, 33(10), 1212-1216. DOI: 10.1016/j.joen.2007.07.007
- Arsham, H. (1994). *The science of making decisions*, The methodology of OR/MS/DS/SS. Available from: <http://home.ubalt.edu/ntsbarsh/opre640/opre640.htm#normaDecscience>
- Bahia, M. G., Melo, M. C., & Buono, V. T. (2008). Influence of cyclic torsional loading on the fatigue resistance of K3 instruments. *International Endodontic Journal*, 41(10), 883-891. DOI: 10.1111/j.1365-2591.2008.01449.x
- Bhagabati, N., Yadav, S., & Talwar, S. (2012). An in vitro cyclic fatigue analysis of different endodontic nickel-titanium rotary instruments. *Journal of Endodontics*, 38(4), 515-518. DOI: 10.1016/j.joen.2011.12.034
- Boessler, C., Paque, F., & Peters, O. A. (2009). The effect of electropolishing on torque and force during simulated root canal preparation with ProTaper shaping files. *Journal of Endodontics*, 35(1), 102-106. DOI: 10.1016/j.joen.2008.09.008
- Braga, L. C., Magalhaes, R.R.S., Nakagawa, R.K.L., Puente, C.G., Bouno, V.T.L., & Bahia, M.G.A. (2013). Physical and mechanical properties of twisted or ground nickel-titanium instruments. *International Endodontic Journal*, 46(5), 458-466. DOI: 10.1111/iej.12011
- Broome & Willis (2007). Competing paradigms and health research. In *Researching health, qualitative, quantitative and mixed methods*. Saks, M., & Alsop, J. London. Sage
- Cheung, G. S., & Darvell, B. W. (2007). Low-cycle fatigue of NiTi rotary instruments of various cross-sectional shapes. *International Endodontic Journal*, 40(8), 626-632. doi: 10.1111/j.1365-2591.2007.01257.x

- Cheung, G. S. P. (2009). Instrument fracture: mechanisms, removal of fragments, and clinical outcomes. *Endodontic Topics*, 16(1), 1-26. DOI: 10.1111/j.1601-1546.2009.00239.x
- Condorelli, G. G., Bonaccorso, A., Smecca, E., Schafer, E., Cantatore, G., & Tripi, T. R. (2010). Improvement of the fatigue resistance of NiTi endodontic files by surface and bulk modifications. *International Endodontic Journal*, 43(10), 866-873. DOI: 10.1111/j.1365-2591.2010.01759.x
- Drexel, M. J., Selvaduray, G.S., & Pelton, A.R. (2008). The effects of cold working and heat treatment on the properties of nitinol wire. *Proceedings of the International Conference on Shape Memory and Superelastic Technologies*, May 7-11 2006, Pacific Grove, California, 447-454. DOI: 10.1361/cp2006smst447
- Ebihara, A. Y., Yahata, Y., Miyara, K., Nakano, K., Hayashi, Y., & Suda, H. (2011). Heat treatment of nickel-titanium rotary endodontic instruments: effects on bending properties and shaping abilities. *International Endodontic Journal*, 44(9), 843-849. DOI: 10.1111/j.1365-2591.2011.01891.x
- Figueiredo, A. M., Modenesi, P., & Buono, V. (2009). Low cycle fatigue life of superelastic NiTi wires. *International Journal of Fatigue*, 31(4), 751-758. DOI: 10.1016/j.ijfatigue.2008.03.014
- Gambarini, G., Plotino, G., Al Sudani, D., Grande, N. M., De Luca, M., & Testarelli, L. (2011). Mechanical properties of nickel-titanium rotary instruments produced with a new manufacturing technique. *International Endodontic Journal*, 44(4), 337-341. DOI: 10.1111/j.1365-2591.2010.01835.x
- Grande, N. M., Plotino, G., Pecci, R., Malagnino, V. A., & Somma, F. (2006). Cyclic fatigue resistance and three-dimensional analysis of instruments from two nickel-titanium rotary systems. *International Endodontic Journal*, 39(10), 755-763. DOI: 10.1111/j.1365-2591.2006.01143.x

- Gutmann, J. L., & Gao, Y. (2012). Alteration in the inherent metallic and surface properties of nickel-titanium root canal instruments to enhance performance, durability and safety: a focused review. *International Endodontic Journal*, *45*(2), 113-128. DOI: 10.1111/j.1365-2591.2011.01957.x
- Harlan, A. L., Nicholls, J.I., & Steiner, J.C. (1996). A comparison of curved canal instrumentation using nickel titanium or stainless steel files with balanced-force technique. *Journal of Endodontics*, *22*(8), 410-413.
- Hargreaves, K., & Cohen, S. (2011). *Pathways of the pulp* (10th ed.). Mosby Elsevier. The most common preparation errors (p318), deformation of endodontic instruments made from nickel titanium alloy (p299).
- Inan, U., Aydin, C., & Tunca, Y. M. (2007). Cyclic fatigue of ProTaper rotary nickel-titanium instruments in artificial canals with 2 different radii of curvature. *Oral Surgery, Oral Medicine, Oral Pathology, Oral Radiology, and Endodontics*, *104*(6), 837-840. DOI: 10.1016/j.tripleo.2007.06.019
- Jamleh, A., Kobayashi, C., Yayata, Y., Ebihara, A., & Suda, H. (2012). Deflecting load of nickel titanium rotary instruments during cyclic fatigue. *Dental Materials Journal*, *31*(3), 389-393. doi: 10.4012/dmj.2011-233
- Kim, H. C., Yum, J., Hur, B., & Cheung, G. S. (2010). Cyclic fatigue and fracture characteristics of ground and twisted nickel-titanium rotary files. *Journal of Endodontics*, *36*(1), 147-152. DOI: 10.1016/j.joen.2009.09.037
- Kocich, R., Szurman, I., & Kurska, M. (2013). *Shape Memory Alloys - Processing, Characterization and Applications*. The Methods of Preparation of Ti-Ni-X Alloys and their Forming. InTech, DOI: 10.5772/50067. Available from: <http://www.intechopen.com/books/shape-memory-alloys-processing-characterization-and-applications/the-methods-of-preparation-of-ti-ni-x-alloys-and-their-forming>

- Larsen, C. M., Watanabe, I., Glickman, G. N., & He, J. (2009). Cyclic fatigue analysis of a new generation of nickel titanium rotary instruments. *Journal of Endodontics*, 35(3), 401-403. DOI: 10.1016/j.joen.2008.12.010
- Lee, M., Versluis, A., Kim, B., Lee, C., Hur, B., & Kim, H. (2011). Correlation between experimental cyclic fatigue resistance and numerical stress analysis for nickel-titanium rotary files. *Journal of Endodontics*, 37(8), 1152-1157. DOI: 10.1016/j.joen.2011.03.025
- Lee, W., Song, M., Kim, E., Lee, H., & Kim, H. (2012). A survey of experience-based preference of nickel-titanium rotary files and incidence of fracture among general dentists. *Restorative Dentistry and Endodontics*, 37(4), 201-206. DOI: 10.5395/rde.2012.37.4.201
- Leroy, A. M., Bahia, M.B, Ehrlacher, A.; & Buono, V.T. (2012). An analytic mechanical model to describe the response of NiTi rotary endodontic files in a curved root canal. *Materials Science and Engineering C*, 32(6), 1594-1600. DOI: 10.1016/j.msec.2012.04.049
- Lopes, H. P., Ferreira, A. A., Elias, C. N., Moreira, E. J., & Siqueira, D. O. (2009). Influence of rotational speed on the cyclic fatigue of rotary nickel-titanium endodontic instruments. *Journal of Endod*, 35(7), 1013-1016. DOI: 10.1016/j.joen.2009.04.003
- McCabe, J.F., Yan, Z., Al Naimi, O.T., Mahmoud, G., & Rolland, S.L. (2011). Smart materials in dentistry. *Australian Dental Journal*, 56(1), 3-10. DOI: 10.1111/j.1834-7819.2010.01291.x
- McVeigh, C., Vernerey, F., Liu, W.K., & Brinson L.C. (2006). Multiresolution analysis for material design. *Computer Methods in Applied Mechanicals and Engineering*, 195(37), 5053-5076. DOI: 10.1016/j.cma.2005.07.027
- Nakagawa, R. K., Alves, J.L., Buono, T.L., & Bahia, G.A. (2013). Flexibility and torsional behaviour of rotary nickel-titanium PathFile, RaCe ISO 10, Scout RaCe and stainless steel K-File hand instruments. *International Endodontic Journal, Early View Online*, 1-8. DOI: 10.1111/iej.12146
- Obaisi, N.A., Galang, M.T.S., Evans, C.A., Tsay, T.P., Viana, M.G., Lukic, H., & Megremis, S.(2013). Determination of transformation temperature ranges of orthodontic nickel-titanium archwires using the bend and free recovery test. *International Association for Dental*

- Research, Poster Session, Washington State Convention Centre, March 23. Abstract available from: <https://iadr.confex.com/iadr/13iags/webprogram/paper177934.html>
- Oh, S.R., Chang, S.W., Lee, Y., Gu, Y., Son, W.J., Lee, W., . . . Kum., K.Y. (2010). A comparison of nickel-titanium rotary instruments manufactured using different methods and cross-sectional areas: ability to resist cyclic fatigue. *Oral Surgery, Oral Medicine, Oral Pathology, Oral Radiology, and Endodontics*, 109(4), 622-628. DOI: 10.1016/j.tripleo.2009.12.025
- Parashos, P., & Messer, H. H. (2006). Rotary NiTi instrument fracture and its consequences. *Journal of Endodontics*, 32(11), 1031-1043. DOI: 10.1016/j.joen.2006.06.008
- Patel, M. M. (2007). Characterizing fatigue response of nickel-titanium alloys by rotary beam testing. *Journal of ASTM International*, 4(6), 1-11. doi: 10.1520/JAI100390
- Pelton, A. R., Russell, S.M., & DiCello, J. (2003). The physical properties of Nitinol for medical applications. *Journal of Metals*, 55(5), 33-37. DOI: 10.1007/s11837-003-0243-3
- Peters, O. A., Gluskin, A.K., Weiss, R.A., & Han, J.T. (2012). An in vitro assessment of the physical properties of novel Hyflex nickel-titanium rotary instruments. *International Endodontic Journal*, 45(11), 1027-1034. DOI: 10.1111/j.1365-2591.2012.02067.x
- Plotino, G., Grande, N. M., Cordaro, M., Testarelli, L., & Gambarini, G. (2009). A review of cyclic fatigue testing of nickel-titanium rotary instruments. *Journal of Endodontics*, 35(11), 1469-1476. DOI: 10.1016/j.joen.2009.06.015
- Plotino, G., Grande, N. M., Cordaro, M., Testarelli, L., & Gambarini, G. (2010). Influence of the shape of artificial canals on the fatigue resistance of NiTi rotary instruments. *International Endodontic Journal*, 43(1), 69-75. DOI: 10.1111/j.1365-2591.2009.01641.x
- Plotino, G., Grande, N. M., Mazza, C., Petrovic, R., & Gambarini, T. (2010). Influence of size and taper of artificial canals on the trajectory of NiTi rotary instruments in cyclic fatigue studies. *Oral Surgery, Oral Medicine, Oral Pathology, Oral Radiology, and Endodontics*, 109(1), e60-66. DOI: 10.1016/j.tripleo.2009.08.009

- Plotino, G., Grande, N. M., Melo, M. C., Bahia, M. G., Testarelli, L., & Gambarini, G. (2010). Cyclic fatigue of NiTi rotary instruments in a simulated apical abrupt curvature. *International Endodontic Journal*, 43(3), 226-230. DOI: 10.1111/j.1365-2591.2009.01668.x
- Rhodes, J.S.(2006) *Advanced endodontics Clinical retreatment and surgery* (1<sup>st</sup> ed.) Taylor & Francis. Rationale for endodontic retreatment p.6.
- Robertson, S. W., Pelton, A.R., & Ritchie, R.O. (2012). Mechanical fatigue and fracture of nitinol. *International Materials Reviews*, 57(1), 1-36. DOI: 10.1179/1743280411Y.0000000009
- Rodrigues, R.C., Lopes, H.P., Elias, L.N., Amaral, G., Vieira, V.T., & De Martin, A.S.(2011). Influence of different manufacturing methods on the cyclic fatigue of rotary nickel-titanium endodontic instruments. *Journal of Endodontics*, 37(11), 1553-1557. DOI: 10.1016/j.joen.2011.08.011
- Schafer, E., Schulzbongert, U., & Tulus, G. (2004). Comparison of Hand Stainless Steel and Nickel Titanium Rotary Instrumentation: A Clinical Study. *Journal of Endodontics*, 30(6), 432-435. DOI: 10.1097/00004770-200406000-00014
- Schafer, E., & Tepel, J. (2001). Relationship between design features of endodontic instruments and their properties. Part 3. Resistance to bending and fracture. *Journal of Endodontics*, 27(4), 299-303. DOI: 10.1097/00004770-200104000-00018
- Shaw, J. A. (2000). Simulations in localised thermo-mechanical behaviour in a NiTi shape memory alloy. *International Journal of Plasticity* (16), 541-562.  
Available from: <http://www.engin.umich.edu/aero/people/files/simulation-sma>
- Shaw, J. A., Churchill, C.B., & Iadicola, M.A. (2008). Tips and tricks for characterizing shape memory alloy wire: part 1- differential scanning calorimetry and basic phenomena *Experimental Techniques* 32(5), 55-62. DOI: 10.1111/j.1747-1567.2008.00410.x
- Shen, Y., Qian, W., Abtin, H., Gao, Y., & Haapasalo, M. (2011). Fatigue Testing of Controlled Memory Wire Nickel-Titanium Rotary Instruments. *Journal of Endodontics*, 37(7), 997-1001. DOI: 10.1016/j.joen.2011.03.023

- Shen, Y., Qian, W., Abtin, H., Gao, Y., & Haapasalo, M. (2012). Effect of environment on fatigue failure of controlled memory wire nickel-titanium rotary instruments. *Journal of Endodontics*, 38(3), 376-380. DOI: 10.1016/j.joen.2011.12.002
- Shen, Y., Zhou, H. M., Zheng, Y. F., Campbell, L., Peng, B., & Haapasalo, M. (2011). Metallurgical characterization of controlled memory wire nickel-titanium rotary instruments. *Journal of Endodontics*, 37(11), 1566-1571. DOI: 10.1016/j.joen.2011.08.005
- Shen, Y., Coil, J.M., Zhou, H., Zheng, Y., & Haapasalo, M. (2013). HyFlex nickel-titanium rotary instruments after clinical use: metallurgical properties. *International Endodontic Journal*, 46(8), 720-729. DOI: 10.1111/iej.12049
- Shen, Y., Zhou, H., Zheng, Y., Peng, B., & Haapasalo, M. (2013). Current challenges and concepts of the thermomechanical treatment of nickel-titanium instruments. *Journal of Endodontics*, 39(2), 163-172. DOI: 10.1016/j.joen.2012.11.005
- Stoeckel, D., & Yu, W. (1991). Superelastic Ni-Ti wire. *Wire Journal International*(March), 45-50. Available from: <http://www.nitinol.com/wp-content/uploads/2012/01/056.pdf>
- Testarelli, L., Plotino, G., Al-Sudani, D., Vincenzi, V., Giansiracusa, A., Grande, N.M., & Gambarini, G. (2011). Bending properties of a new nickel-titanium alloy with a lower percent by weight of nickel. *Journal of Endodontics*, 37(9), 1293-1295. DOI: 10.1016/j.joen.2011.05.023
- Topuz, O., Aydin, C., Uzun, O., Inan, U., & Tunca, A. (2008). Structural effects of sodium hypochlorite solution on RaCe rotary nickel-titanium instruments: an atomic force microscopy study. *Oral Surgery, Oral Medicine, Oral Pathology, Oral Radiology, and Endodontics*, 105(5), 661-665. DOI: 10.1016/j.tripleo.2007.11.006
- Wu, R. C., & Chung, C.Y. (2012). Differential scanning calorimetric (DSC) analysis of rotary nickel-titanium endodontic file. *Journal of Materials Engineering and Performance*, 21(12), 2515-2518. DOI: 10.1007/s11665-012-0269-1
- Young, G. R., Parashos, P., & Messer, H.H. (2007). The principles of techniques for cleaning root canals. *Australian Dental Journal*, 52(1), 52-63. Available from: <http://onlinelibrary.wiley.com/doi/10.1111/j.1834-7819.2007.tb00526.x/pdf>



- Young, J. M., & Van Vliet, K.J. . (2005). Predicting in vivo failure of pseudoelastic NiTi devices under low cycle, high amplitude fatigue. *Journal of Biomedical Materials Research Part B: Applied Biomaterials*, 72B(1), 17-26. DOI: 10.1002/jbm.b.30113
- Zhang, E. W., Cheung, G. S., & Zheng, Y. F. (2010). Influence of cross-sectional design and dimension on mechanical behavior of nickel-titanium instruments under torsion and bending: a numerical analysis. *Journal of Endodontics*, 36(8), 1394-1398. DOI: 10.1016/j.joen.2010.04.017
- Zhou, H., Shen, Y., Zheng, W., Li, L., Zheng, Y., & Haapasalo, M. (2012). Mechanical properties of controlled memory and superelastic nickel-titanium wires used in the manufacture of rotary endodontic instruments. *Journal of Endodontics*, 38(11), 1535-1540. DOI: 10.1016/j.joen.2012.07.006
- Zinelis, S., Eliades, T., & Eliades, G. (2010). A metallurgical characterization of ten endodontic Ni-Ti instruments: assessing the clinical relevance of shape memory and superelastic properties of Ni-Ti endodontic instruments. *International Endodontic Journal*, 43(2), 125-134. DOI: 10.1111/j.1365-2591.2009.01651.x
- Zinelis, S. Darabara, M., Takase, T., Ogane, K., & Papadimitriou, G.D. (2007). The effect of thermal treatment on the resistance of nickel-titanium rotary files in cyclic fatigue. *Oral Surgery, Oral Medicine, Oral Pathology, Oral Radiology, and Endodontics*, 103(6), 843-847. DOI: 10.1016/j.tripleo.2006.12.026

## Appendix A

Specifications of tempered BA2 tool steel used for fabricating the test block. After tempering hardness is given as  $\geq 60$  on the Rockwell C Scale Hardness (HRC) in table 5. Conversion of HRC gives a Vickers hardness of  $\geq 740$  from table 6.

Table 14. Rockwell C Scale hardness of BA2 tool steel (from [www.steel-grades.co.uk](http://www.steel-grades.co.uk)).

Table 15. Conversion table for Rockwell Hardness C to Vickers Hardness (from [www.taylorspecialsteels.co.uk](http://www.taylorspecialsteels.co.uk)).

## Appendix B

Geometry of the artificial canal.

Figure 35. PDF showing start and finish width of the canal (From Waveney Precision).

Figure 36. Annotated CAD screenshot of the data used to manufacture the copper die for electrical discharge machining of the BA2 steel block to a depth of 2mm (screenshot from Waveney Precision.).

The general location of maximum strain on the instruments is in the middle of the curvature. This is given by calculating the average length of the curved section first. This is the circumference of a circle with a 5mm radius and divided by 4, as it is a 90° radius of

curvature, this is equal to 7.85mm. The middle point is then 3.925mm. Adding the initial 3mm gives a point around the 7mm mark. Most files failed at around this point.

### Appendix C

Converted data in the form of number of rotations to failure ( $N_f$ ) as entered into SPSS™. The first 47 data values are for HyFlexCM™ (label 1.00). Data values from 48 -96 represent RaCe™ instruments (label 2.00)

1	1.00	69.16	30	1.00	73.91
2	1.00	117.74	31	1.00	78.91
3	1.00	142.41	32	1.00	77.25
4	1.00	151.16	33	1.00	88.74
5	1.00	70.91	34	1.00	88.66
6	1.00	51.33	35	1.00	110.33
7	1.00	43.08	36	1.00	94.82
8	1.00	107.50	37	1.00	119.58
9	1.00	112.25	38	1.00	87.33
10	1.00	86.50	39	1.00	119.75
11	1.00	63.25	40	1.00	78.33
12	1.00	54.50	41	1.00	47.91
13	1.00	95.83	42	1.00	81.83
14	1.00	151.66	43	1.00	90.25
15	1.00	140.00	44	1.00	87.58
16	1.00	66.91	45	1.00	105.75
17	1.00	174.24	46	1.00	102.66
18	1.00	154.16	47	1.00	86.08
19	1.00	111.66	48	2.00	94.41
20	1.00	45.50	49	2.00	112.83
21	1.00	41.57	50	2.00	103.50
22	1.00	190.16	51	2.00	71.50
23	1.00	132.66	52	2.00	72.58
24	1.00	81.41	53	2.00	89.75
25	1.00	75.08	54	2.00	106.16
26	1.00	82.41	55	2.00	68.83
27	1.00	91.50	56	2.00	92.33
28	1.00	84.16	57	2.00	95.58
29	1.00	110.91	58	2.00	96.83
30	1.00	73.91	59	2.00	8.50

60	2.00	89.41
61	2.00	40.75
62	2.00	101.33
63	2.00	94.83
64	2.00	91.25
65	2.00	106.50
66	2.00	124.25
67	2.00	118.82
68	2.00	145.58
69	2.00	89.83
70	2.00	126.83
71	2.00	119.16
72	2.00	109.91
73	2.00	109.88
74	2.00	116.75
75	2.00	115.58
76	2.00	103.00
77	2.00	95.16
78	2.00	96.75
79	2.00	112.25
80	2.00	116.50
81	2.00	111.08
82	2.00	97.41
83	2.00	84.41
84	2.00	112.41
85	2.00	121.25
86	2.00	84.08
87	2.00	143.91
88	2.00	97.33
89	2.00	96.33
90	2.00	125.83
91	2.00	106.08
92	2.00	72.08
93	2.00	72.16
94	2.00	107.08
95	2.00	78.58